NASA MEMO 5-7-59L

NASA

MEMORANDUM

FLIGHT INVESTIGATION OF EFFECTS OF TRANSITION, LANDING APPROACHES, PARTIAL-POWER VERTICAL DESCENTS, AND DROOP-STOP POUNDING ON THE BENDING AND TORSIONAL MOMENTS ENCOUNTERED BY A HELICOPTER ROTOR BLADE

By LeRoy H. Ludi

Langley Research Center
Langley Field, Va.

NATIONAL AERONAUTICS AND SPACE ADMINISTRATION
WASHINGTON
May 1959

NATIONAL AERONAUTICS AND SPACE ADMINISTRATION

MEMORANDUM 5-7-59L

FLIGHT INVESTIGATION OF EFFECTS OF TRANSITION, LANDING APPROACHES, PARTIAL-POWER VERTICAL DESCENTS, AND DROOP-STOP POUNDING ON THE BENDING AND TORSIONAL MOMENTS ENCOUNTERED BY A HELICOPTER ROTOR BLADE

By LeRoy H. Ludi

SUMMARY

Flight tests have been conducted with a single-rotor helicopter, one blade of which was equipped at 14 percent and 40 percent of the blade radius with strain gages calibrated to measure moments rather than stresses, to determine the effects of transition, landing approaches, and partial-power vertical descents on the rotor-blade bending and torsional moments. In addition, ground tests were conducted to determine the effects of static droop-stop pounding on the rotor-blade moments.

The results indicate that partial-power vertical descents and landing approaches produce rotor-blade moments that are higher than the moments encountered in any other flight condition investigated to date with this equipment. Decelerating through the transition region in level flight was found to result in higher vibratory moments than accelerating through this region. Deliberately induced static droop-stop pounding produced flapwise bending moments at the 14-percent-radius station which were as high as the moments experienced in landing approaches and partial-power vertical descents.

INTRODUCTION

The problem of designing structurally efficient helicopter rotor blades requires a knowledge of the periodic moments encountered by the blades during various flight conditions. Information concerning these periodic moments, in conjunction with the percentage of time spent in the various conditions, is necessary for rotor-blade service life predictions. Reference 1 showed that atmospheric turbulence and moderate control motions did not produce additional periodic blade moments, except when accompanied by center-of-gravity accelerations, that were significant

to fatigue calculations during the principal part of the flying time. This information in reference 1 shows that it is permissible to use the percentage of time spent in various flight conditions, as determined by an NACA helicopter VGHN recorder in conjunction with prototype strain measurements, as a basis for that portion of the cumulative fatigue analysis that covers the principal part of the flying time. The results of reference 2 indicated that retreating-blade stall can produce large increases in periodic blade moments during high-speed flight and pull-up maneuvers.

Additional tests were conducted to study specific flight conditions which were expected to produce severe periodic rotor blade moments that would be of interest in the design of the various helicopter components. Several of these flight conditions are decelerating or accelerating through the transition region in level flight, landing approaches, and partial-power vertical descents. These three flight conditions are related by the fact that they encounter changes in the rotor flow characteristics which could result in increased moments. Increased vibrations are also encountered in these flight conditions as shown, for example, in reference 3. In addition to the flight conditions, static droop-stop pounding during rotor operation on the ground also produced some additional periodic blade moments which were of interest. The effects of these flight conditions plus the droop-stop-pounding condition on a helicopter rotor blade are the subject of the present paper. These results will provide an insight into the various conditions that can be expected to produce increased moments so that their effects can be better considered in the design of future helicopter components.

SYMBOLS

v_{hov}	induced velocity in hovering, $\sqrt{\frac{T}{2\rho\pi R^2}}$, fps
T	rotor thrust, lb
ρ	mass density of air, slugs/cu ft
R	blade radius, ft
V_v	vertical velocity, positive when upward, fps
V_i	indicated airspeed, $V\sqrt{\frac{\rho}{\rho_0}}$, knots
V	true airspeed, knots

ρ_0 standard mass density of air, 0.002378 slug/cu ft

$\bar{V}$ nondimensional vertical velocity, $\frac{V_v}{v_{hov}}$

$\Delta B_{1,s}$ change in longitudinal cyclic pitch, positive when stick moved forward, deg

TEST EQUIPMENT AND INSTRUMENTATION

The single-rotor helicopter used in this investigation is shown in figure 1, and the rotor principal dimensions and physical characteristics are given in table I. The main rotor blades are of all-metal construction with a uniform-spar, constant-chord plan form.

Data recording is accomplished by standard NACA recording instruments with synchronized time scales which measure airspeed, altitude, manifold pressure, rotor rotational speed, pilot-control positions, angular velocities about the three principal inertia axes, and center-of-gravity acceleration.

Information on the moments encountered by the rotor blade is obtained by the use of strain-gage bridges calibrated to measure moments rather than stresses and located on the spar of one blade at 14 percent and 40 percent of the blade radius as shown in figure 2 of reference 1. Two spanwise stations were considered adequate for this investigation because only comparative flight results were desired and because the stations were carefully chosen to provide response from the first three bending modes. The strain gages at the 40-percent-radius station measure only flapwise bending moments, whereas the strain gages at the 14-percent-radius station measure flapwise and chordwise bending and torsional moments. (These moments are hereinafter referred to as 40-percent flapwise bending moments, 14-percent chordwise bending moments, and so forth.) Chordwise-bending-moment information was not available during all of the tests because a malfunction of the chordwise-bending-moment bridge required that it be removed from the recording circuit.

TEST PROCEDURE

The procedures used for investigating the various conditions are outlined in the following sections. The data were reduced by the same methods described in reference 1.

Transition

Transition is a term generally used to refer to a flight condition intermediate between hovering and the speed for minimum power and is defined herein as the speed region from hovering to 50 knots where the periodic moments reach a maximum. To investigate the effects of passing through the transition region in either a decelerating or an accelerating condition, tests were made in level flight (altitude deviations less than ±25 feet) both in ground effect and out of ground effect. The tests in the decelerating condition were initiated at some speed above the transition region, and the helicopter was slowly decelerated from this initial speed to hovering while maintaining level flight. For tests in the accelerating condition, the helicopter was slowly accelerated from hovering to an indicated airspeed of approximately 50 knots while maintaining level flight. Selected portions of the time histories for various airspeeds were chosen for analysis to determine how the moments varied with airspeed.

Landing Approaches

The moments encountered during landing approaches were determined by performing approaches which terminated in a hovering condition in ground effect. Two types of landing approaches were investigated. The first type was a normal approach where the speed prior to the landing flare was above 30 knots (hereinafter referred to as a normal approach). Rotor inertia is mostly used to check the rate of descent during the normal approach. The second type was an approach where the speed prior to the landing flare was below 30 knots (hereinafter referred to as a low-speed approach). Engine power is mostly used to check the rate of descent during the low-speed approach. In order to determine the moment variation during the approaches, cycles were analyzed at various airspeeds for each approach.

Partial-Power Vertical Descents

Three basic flow states exist for the rotor in vertical flight: the normal working state, the vortex-ring state, and the windmill-brake state (ref. 4). In order to determine the moments experienced by the rotor during the vortex-ring state and windmill-brake state, partial-power vertical descents were performed. The rates of descent ranged from approximately 200 ft/min to approximately 2,200 ft/min during these tests. In order to generalize the data, the rates of descent are nondimensionalized by dividing by the induced velocity in hovering v_{hov} to account for disk loading and density. The rates of descent were held constant throughout the various tests with the exception of rates of descent that produced large amounts of recirculating flows. Under these conditions, the pilot

had little control over the rate of descent. All the tests were performed with $V_i = 0$. Numerous moment cycles were analyzed at the various rates of descent.

Droop-Stop Pounding

Static droop-stop pounding can inadvertently occur during rotor operation on the ground in strong gusty winds and, therefore, is of interest in a blade-moment study. Static-droop-stop-pounding tests were made on the ground with the rotor turning at a speed just below the "sling out" speed of the centrifugal droop stops (approximately 130 rpm). A moderate collective pitch setting was maintained so that the rotor blade would be off the droop stops during a revolution. The cyclic stick was then slowly and continuously moved so that the blades contacted the stops during part of the revolution. The droop-stop pounding was terminated at the discretion of the pilot. Cycles were analyzed both when the blade was off the droop stops and when it was on the droop stops.

RESULTS AND DISCUSSION

The vibratory moments encountered by a helicopter rotor blade during transition, landing approaches, partial-power vertical descents, and static droop-stop pounding are presented, analyzed, and compared with those obtained in previous tests presented in references 1 and 2. Harmonic analyses are presented to illustrate which harmonics are most affected by these selected conditions.

Sample Traces

Figure 2 shows representative samples of the traces obtained during the four conditions that were investigated. These traces are presented for illustrative purposes and are analyzed in detail in a subsequent section. For the transition and landing-approach conditions, traces at two different airspeeds are presented for each condition. In order to illustrate the variations during partial-power vertical descents, the traces for three different rates of descent are shown. The droop-stop-pounding traces are presented for the instant at which pounding first begins and for the time at which the pounding is the maximum investigated. Flapping-motion traces are also shown in figure 2(d).

Maximum Vibratory Moments

The maximum vibratory moments encountered during the selected conditions were calculated by using one-half the peak-to-peak amplitude.

Transition.- The effects of the transition region on the rotor blade maximum vibratory moments are shown in figure 3. In this figure, the rotor blade moments are plotted as a function of indicated airspeed for both the decelerating and the accelerating conditions. The tests were conducted both in ground effect and out of ground effect. The 14-percent chordwise-bending-moment bridge was inoperative during the accelerating tests.

An inspection of figure 3 shows that, in general, the maximum vibratory moments encountered while decelerating through the transition region (approximately 5,000 inch-pounds for the 40-percent flapwise bending moments) are larger than the moments encountered while accelerating through this region. Figure 3 also shows that ground effect does not have any great effect on the maximum value of the vibratory moments but it does cause a shift in the speed at which the maximum occurs. The increased moments in the transition region are believed to be the result of a change in the flow characteristics through the rotor. One inherent difference between the decelerating and accelerating conditions is that the rotor attitude during the decreasing-speed tests places the rotor closer to the partial-power descent condition.

Landing approaches.- The maximum vibratory moments experienced by the rotor blade during landing approaches are shown in figure 4. In this figure, the rotor-blade moments are plotted as a function of indicated airspeed for both the normal approach and the low-speed approach. Since the results obtained during the landing-approach tests are not readily repeatable, the moments plotted in this figure represent the maximum values obtained during the investigation. The 14-percent chordwise-bending-moment bridge was inoperative during the low-speed approaches.

In general, figure 4 shows that flapwise bending moments as high as 6,500 inch-pounds at the 14-percent-radius station are encountered during the low-speed approaches. The maximum moments, however, occur at the same airspeed during both types of approaches. The maximum moments were found to be approximately two to three times the moments encountered at speeds above 30 knots. The airspeed range in which the maximum moments occur during landing approaches corresponds fairly well with the airspeed range in which the maximum moments occur during deceleration through the transition region. The increased moments encountered in the landing approach are believed to be caused by a change in the air flow similar to that which occurs during deceleration through the transition region. The increased moments during low-speed landing approaches were among the highest encountered in this investigation.

Partial-power vertical descents.- The effect of partial-power vertical descents on the maximum vibratory moments encountered by the rotor blade is shown in figure 5. The rotor-blade moments are plotted as a function of the nondimensional rates of descent in this figure. Since

the moments at a particular rate of descent are not repeatable, the moments plotted in the figure represent the maximum moments encountered in the various descents.

In general, figure 5 shows flapwise moments at the 14-percent-radius station as high as 7,800 inch-pounds in the range from $\bar{V} = -0.4$ to -0.8 which corresponds to a rate-of-descent range from approximately 600 ft/min to 1,200 ft/min. In this range, control was generally poor and required large movements of the controls to keep steady conditions. In addition, the vibration level was generally quite high. This flight condition produced the highest vibratory moments of all the conditions investigated in this series of tests. Furthermore, these moments were higher than those presented in reference 1 for atmospheric turbulence and moderate maneuvers and in reference 2 for retreating-blade stall.

Droop-stop pounding.- The maximum vibratory moments encountered by the rotor blade during static droop-stop pounding as induced on the ground are shown in figure 6. Here the moments are plotted as a function of the change in longitudinal cyclic pitch, with the cyclic pitch at which droop-stop pounding first occurs used as a reference. The test was made with a collective pitch setting of approximately 7°.

Figure 6 shows that the 14-percent flapwise bending moments are affected to a greater extent than are the other moments during the droop-stop pounding. The moments for this station increase from a value of about 2,000 inch-pounds to a value of about 7,500 inch-pounds for a change of longitudinal cyclic pitch of 3.3°. The large increases in moments at the root of the blade are the result of the flapping inertia when the blade impinges on the static droop stop. The moments on the inboard portion of the blade are as high as those produced by landing approaches and partial-power vertical descents. These moments are felt to be an indication of the rate of increase of moments with control displacement if droop-stop pounding is inadvertently permitted, at least for a blade with uniform spar and uniform mass.

Harmonic Analysis of Moment Records

In order to determine the harmonic content of the moment records, 24-point harmonic analyses were performed. As an aid in interpreting these harmonic analyses, the rotor-blade-frequency diagram (fig. 7) is included. This diagram was determined by using the procedures of reference 5 and the measured nonrotating-blade frequencies. An inspection of figure 7 reveals possible resonant amplification of the second and third flapwise bending modes in the normal operating range.

Harmonic analyses for transition, landing approaches, partial-power vertical descents, and static droop-stop pounding are shown in figures 8,

9, 10, and 11, respectively. In all the harmonic-analysis bar graphs, a positive steady-state value indicates (1) for flapwise bending moment, compression in the upper surface of the blade, (2) for chordwise bending moment, compression in the trailing edge of the blade, and (3) for torsional moment, couple tending to rotate the blade leading edge upward. The steady-state values of the chordwise bending and torsional moments were found to be negative in all cases as is shown by minus signs over the steady-state-moment bars.

Transition.- The results for the harmonic analysis of the moments during transition are shown in figure 8. In this figure the various moments at the different stations are presented for the steady state and first 10 harmonics. The moments are shown for two different airspeeds: one that is outside of the transition region and one that is in the transition region. The moments encountered while decelerating through the transition region, which are generally higher than the moments encountered while accelerating through the transition region, are the only ones presented in the figure.

An inspection of figure 8 shows that the flapwise bending moments are those most affected by the transition region. The rapid change in flow characteristics when traversing the transition region are presumably the cause of the increased bending moments shown for most of the harmonics. The large increase in the fifth flapwise harmonic in the transition region indicates the possibility of resonance amplification. These increased harmonic moments illustrate the difficulty of avoiding resonance completely at all frequencies for all flight conditions. They also indicate the necessity of locating the strain gages during prototype, as well as research, testing so as to avoid nodal points for at least the first three bending modes. The 14-percent chordwise bending and torsional moments are generally less affected by the transition region.

Landing approaches.- Figure 9 shows the harmonic analyses of the moments encountered during low-speed landing approaches. These moments are presented since they generally result in maximum values that are higher than those obtained in a normal landing approach. The maximum moments encountered during the final part of the approach are compared with the moments that occurred during the steady or initial part of the approach descent.

In general, increased moments are shown in this figure for the majority of the harmonics during the period where the speed is being reduced for the landing flare. Since there was no appreciable normal acceleration or pitching velocity in the flare during a low-speed approach, the increased moments are felt to be the result of the rapidly changing flow characteristics through the rotor. Possible resonance amplification is again indicated by increased moments for the fifth harmonic.

Partial-power vertical descents.- The effects of partial-power vertical descents on the individual harmonic moments are shown in figure 10. In this figure, the moments are plotted for the following rates of descent: 440 ft/min ($\overline{V}$ = -0.288), 830 ft/min ($\overline{V}$ = -0.544), and 1,490 ft/min ($\overline{V}$ = -0.975).

The figure shows that a rate of descent of 830 ft/min produces some outstanding increases in the harmonic moments, particularly for the flapwise bending moments. These increased moments are associated with the large amount of turbulence produced by the recirculating flow which occurs at this rate of descent. The moments encountered by the blade under these recirculating conditions fluctuate considerably; therefore, the moments in figure 10 represent the maximum moments during the descent. The large increases in the fifth harmonic for the flapwise bending moment indicate the possibility of second-mode resonance amplification.

Droop-stop pounding.- The harmonic moments encountered during static droop-stop pounding are shown in figure 11. The moments presented in this figure are for two values of longitudinal cyclic pitch: one that represents the point where droop-stop pounding first occurs and one that represents the maximum stick deflection attempted.

At the point where the change in longitudinal cyclic stick is equal to 3.3°, figure 11 reveals that the 14-percent flapwise bending moments are those most affected by the stop pounding, the first through fifth harmonics showing the largest increases. The first, second, and third harmonics for this condition experienced bending moments that were larger than those encountered during the other conditions of this investigation. In addition, the 14-percent flapwise steady-state value at $\Delta B_{1,s} = 3.3°$ has a negative sign which indicates an average value of tension in the upper surface of the blade. Mean-value tension in the upper surface of the blade was first encountered when $\Delta B_{1,s} \approx 3°$. The other moments encountered by the rotor do not show any outstanding increases due to droop-stop pounding.

CONCLUSIONS

The flight investigation of the effects of transition, landing approaches, partial-power vertical descents, and droop-stop pounding on the periodic rotor-blade moments of a fully articulated, single-rotor helicopter indicated the following conclusions:

1. For all the flight conditions investigated to date (atmospheric turbulence, moderate maneuvers, retreating-blade stall, transition,

landing approaches, partial-power vertical descents, and static droop-stop pounding), the largest vibratory moments were produced by partial-power vertical descents at zero forward speed. These maximums occurred in the nondimensional-vertical-velocity range from -0.4 to -0.8. Vibratory moments encountered during low-speed landing approaches, although not as high as the moments produced in partial-power vertical descents, also were very high.

2. Vibratory moments encountered while decelerating through the transition region are higher than the vibratory moments encountered while accelerating through the transition region.

3. Static droop-stop pounding, deliberately induced by 3.3° of cyclic stick beyond the initial contact value, during rotor operation on the ground resulted in flapwise vibratory moments at the 14-percent radius station that are as high as those produced by landing approaches and partial-power vertical descents.

Langley Research Center,
National Aeronautics and Space Administration,
Langley Field, Va., February 16, 1959.

REFERENCES

1. Ludi, LeRoy H.: Flight Investigation of Effects of Atmospheric Turbulence and Moderate Maneuvers on Bending and Torsional Moments Encountered by a Helicopter Rotor Blade. NACA TN 4203, 1958.

2. Ludi, LeRoy H.: Flight Investigation of Effects of Retreating-Blade Stall on Bending and Torsional Moments Encountered by a Helicopter Rotor Blade. NACA TN 4254, 1958.

3. Yeates, John E.: Flight Measurements of the Vibration Experienced by a Tandem Helicopter in Transition, Vortex-Ring State, Landing Approach, and Yawed Flight. NACA TN 4409, 1958.

4. Gessow, Alfred, and Myers, Garry C., Jr.: Aerodynamics of the Helicopter. The Macmillan Co., c.1952.

5. Yntema, Robert T.: Simplified Procedures and Charts for the Rapid Estimation of Bending Frequencies of Rotating Beams. NACA TN 3459, 1955. (Supersedes NACA RM L54G02.)

TABLE I.- PRINCIPAL DIMENSIONS AND PHYSICAL CHARACTERISTICS

OF TEST HELICOPTER AND ROTOR

Gross weight, lb	6,900
Number of blades	3
Rotor-blade radius, ft	26.5
Flapping-hinge offset, ft	0.75
Weight of blades (approximate), lb/blade	136
Main rotor blade:	
Type	All metal, constant chord
Twist, deg	-8
Airfoil section	NACA 0012
Blade chord, ft	1.368
Rotor solidity, σ	0.0493
Approximate rotor-blade mass constant, γ	11
Design rotor-blade tip speed, ft/sec	538
Disk loading, lb/sq ft	3.12
Design rotor angular velocity, radians/sec	20.3
Center of gravity, inches from reference datum (reference datum 14.5 inches forward of nose)	129.6

Figure 1.- Test helicopter. L-84196

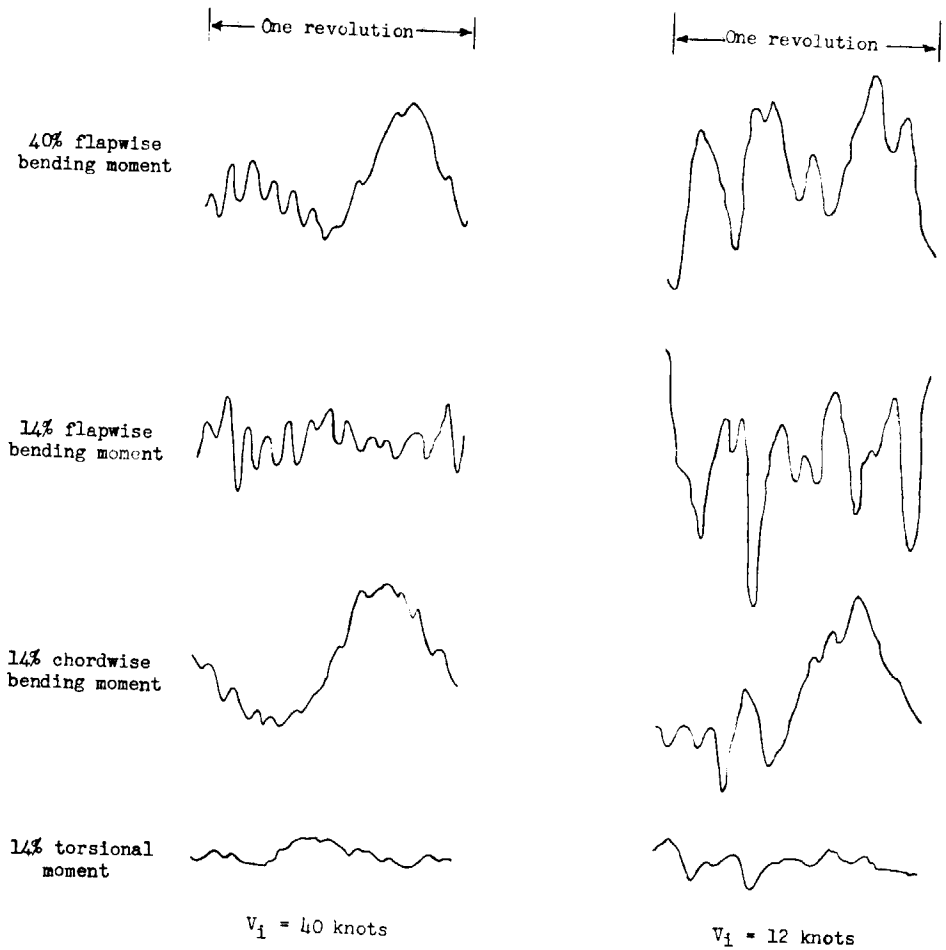

(a) Decelerating through transition region (in ground effect).

Figure 2.- Typical time histories of rotor-blade moments obtained during the various conditions investigated.

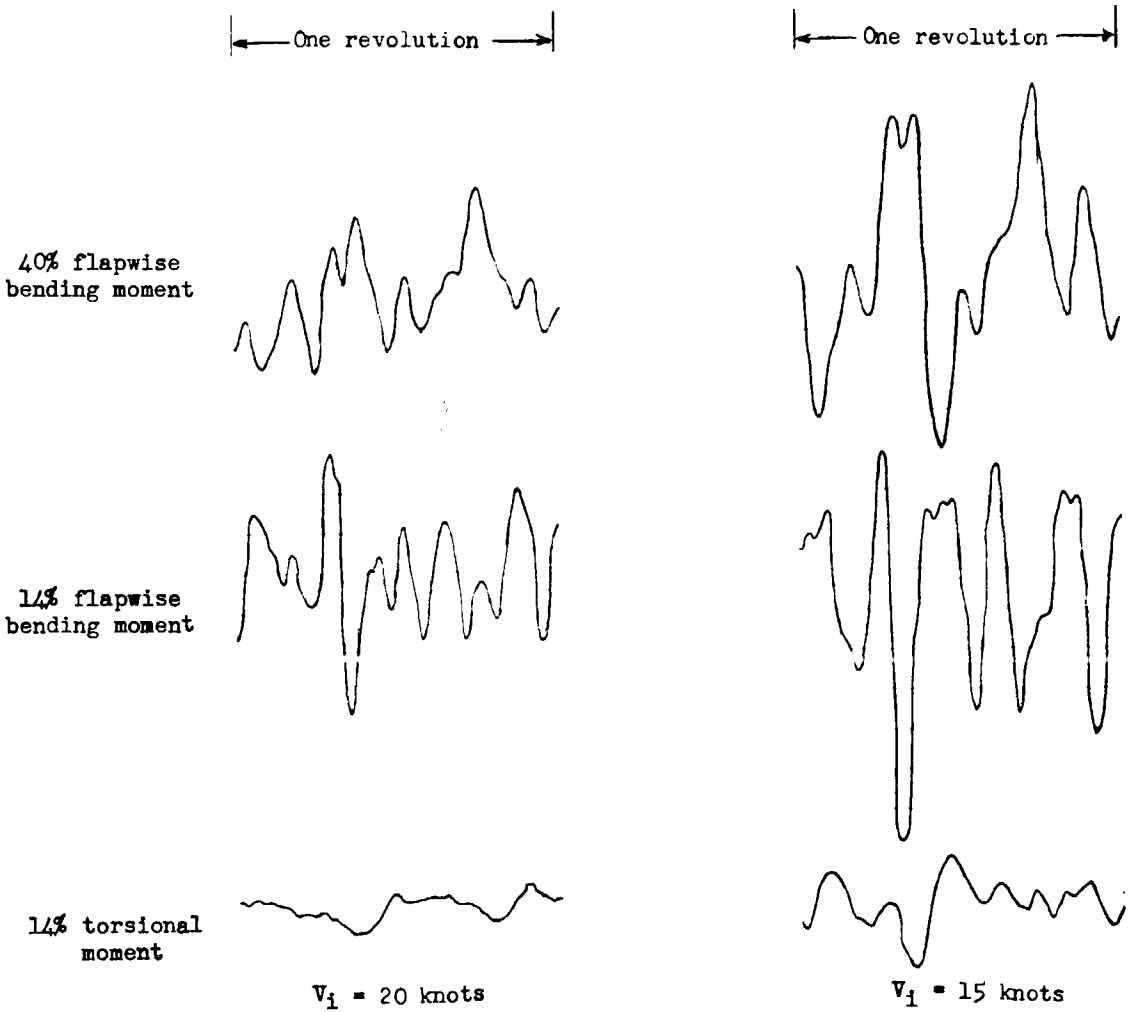

(b) Low-speed landing approach.

Figure 2.- Continued.

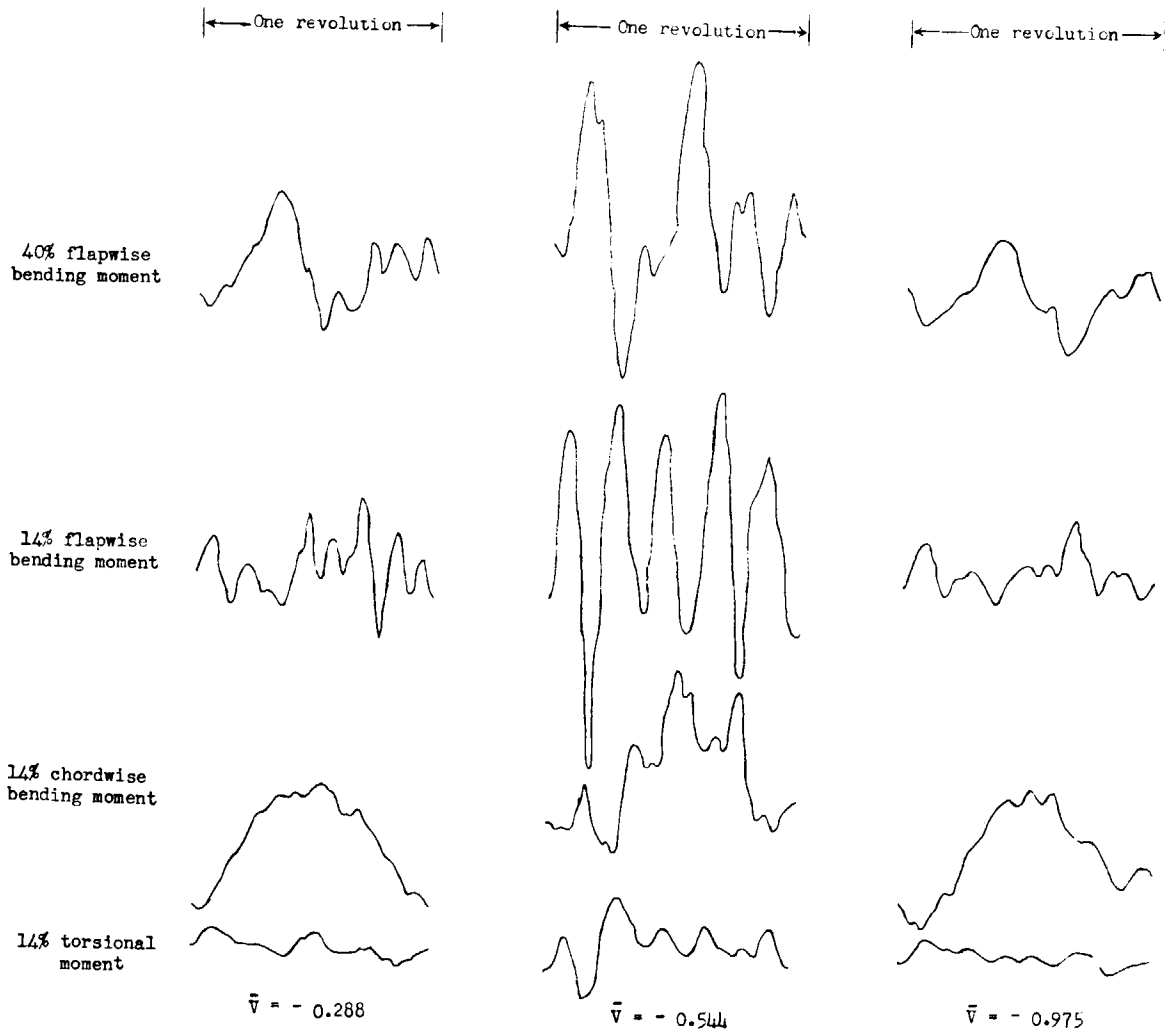

(c) Partial-power vertical descents.

Figure 2.- Continued.

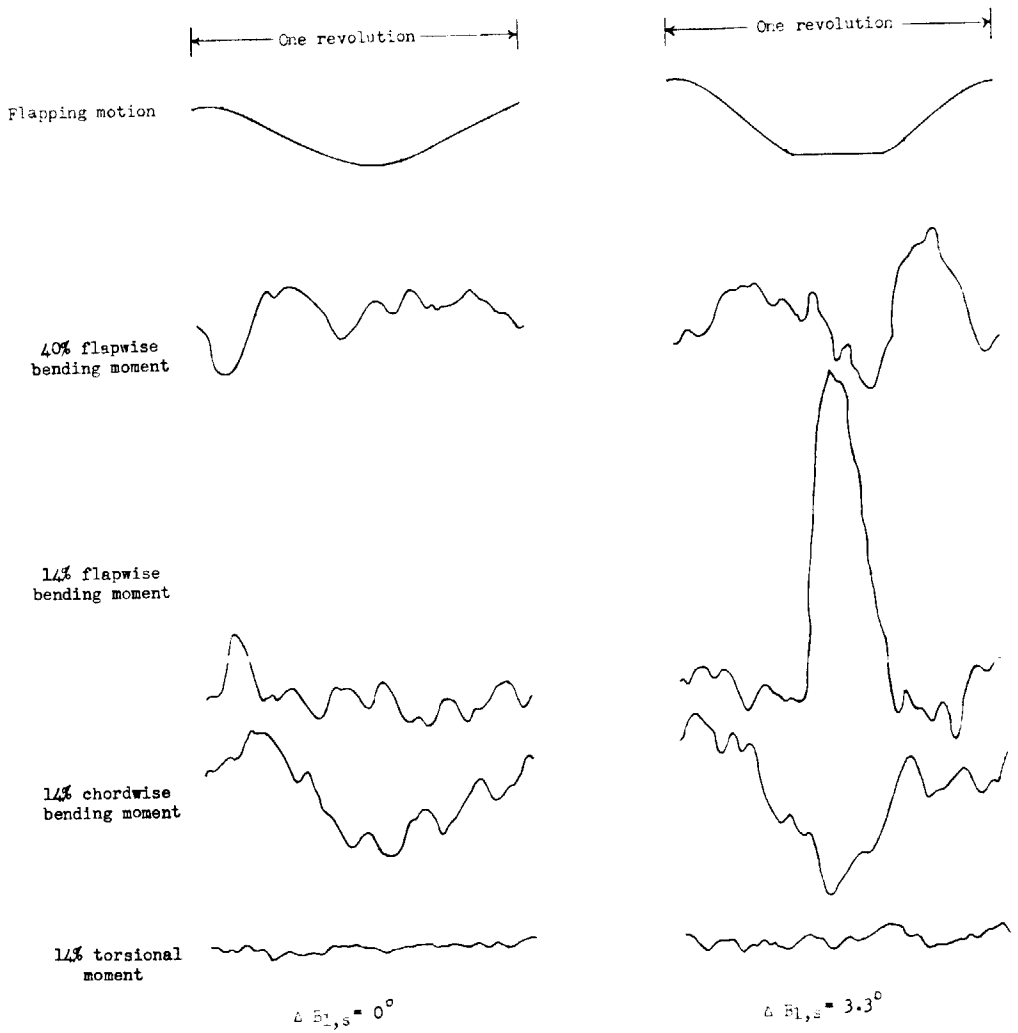

(d) Droop-stop pounding.

Figure 2.- Concluded.

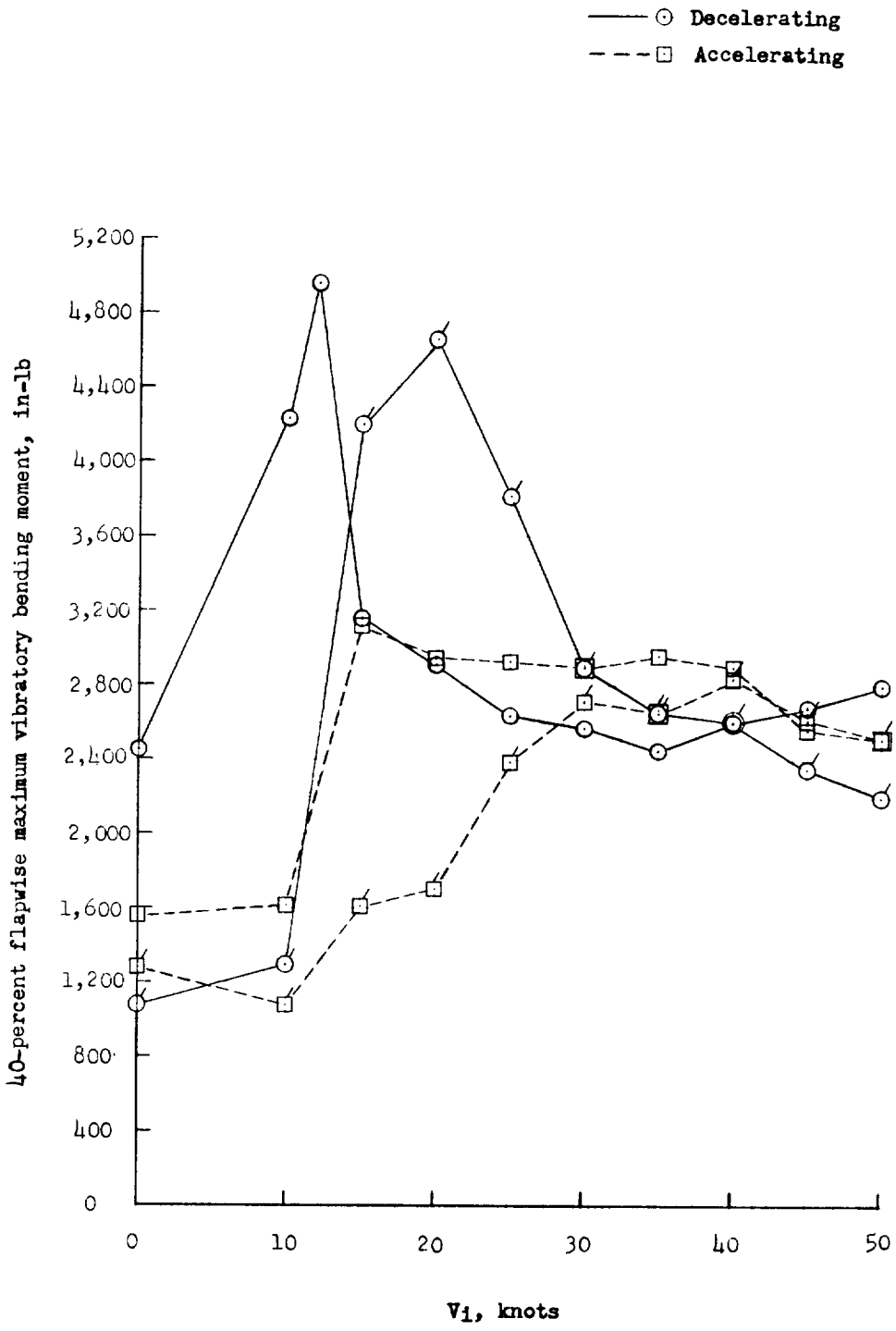

Figure 3.- Effects of transition on the maximum vibratory moments. Flagged symbols denote tests out of ground effect.

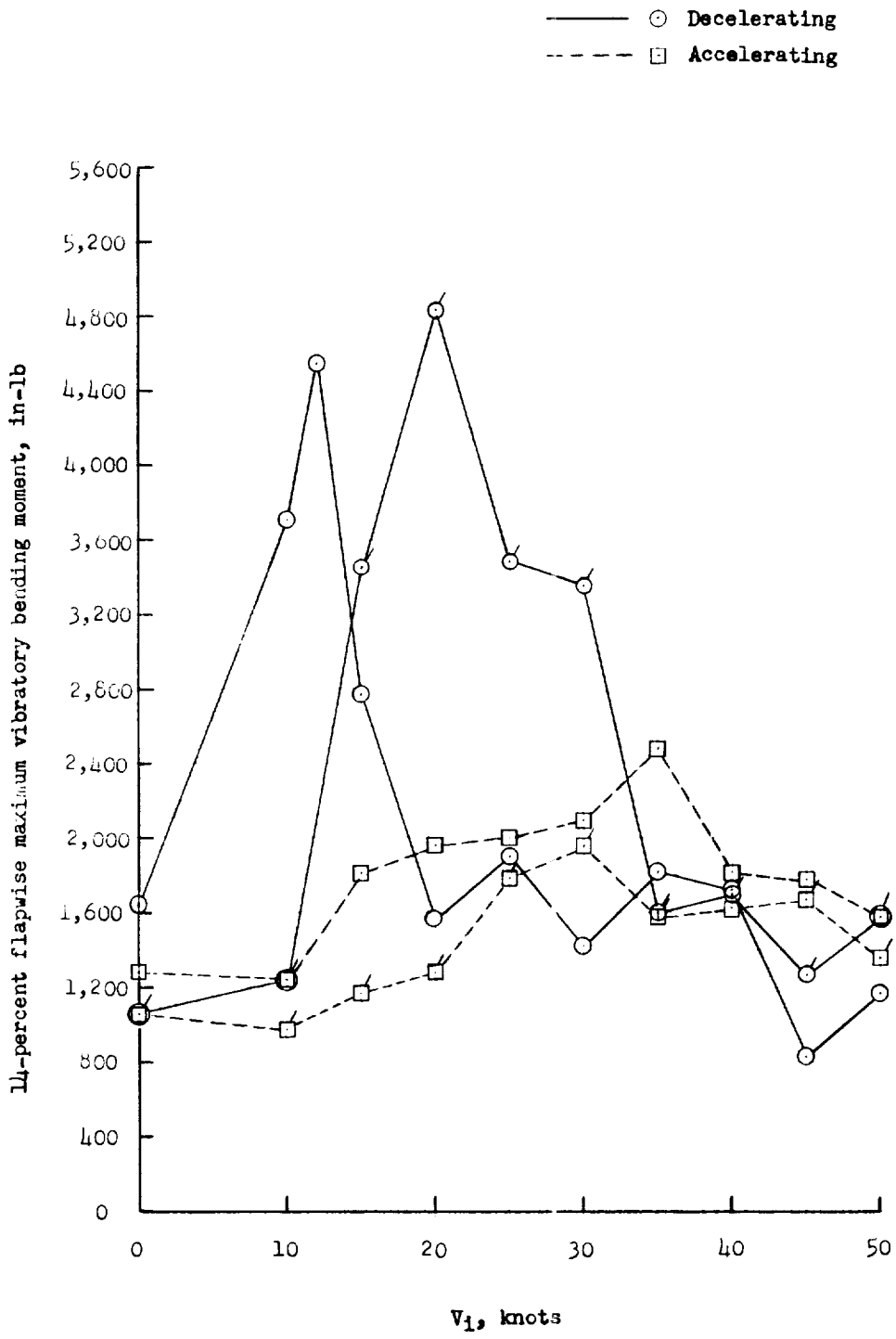

Figure 3.- Continued.

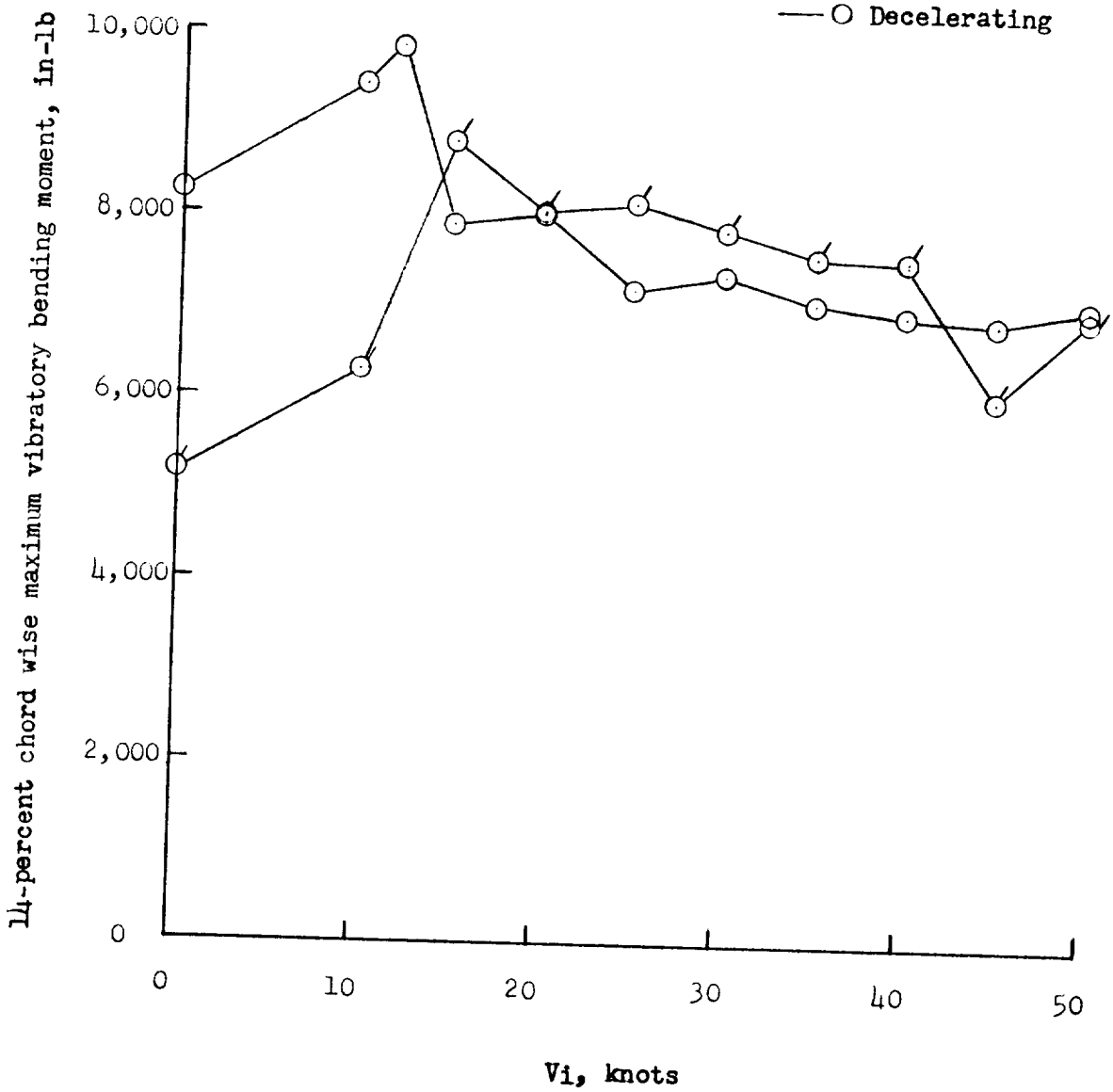

Figure 3.- Continued.

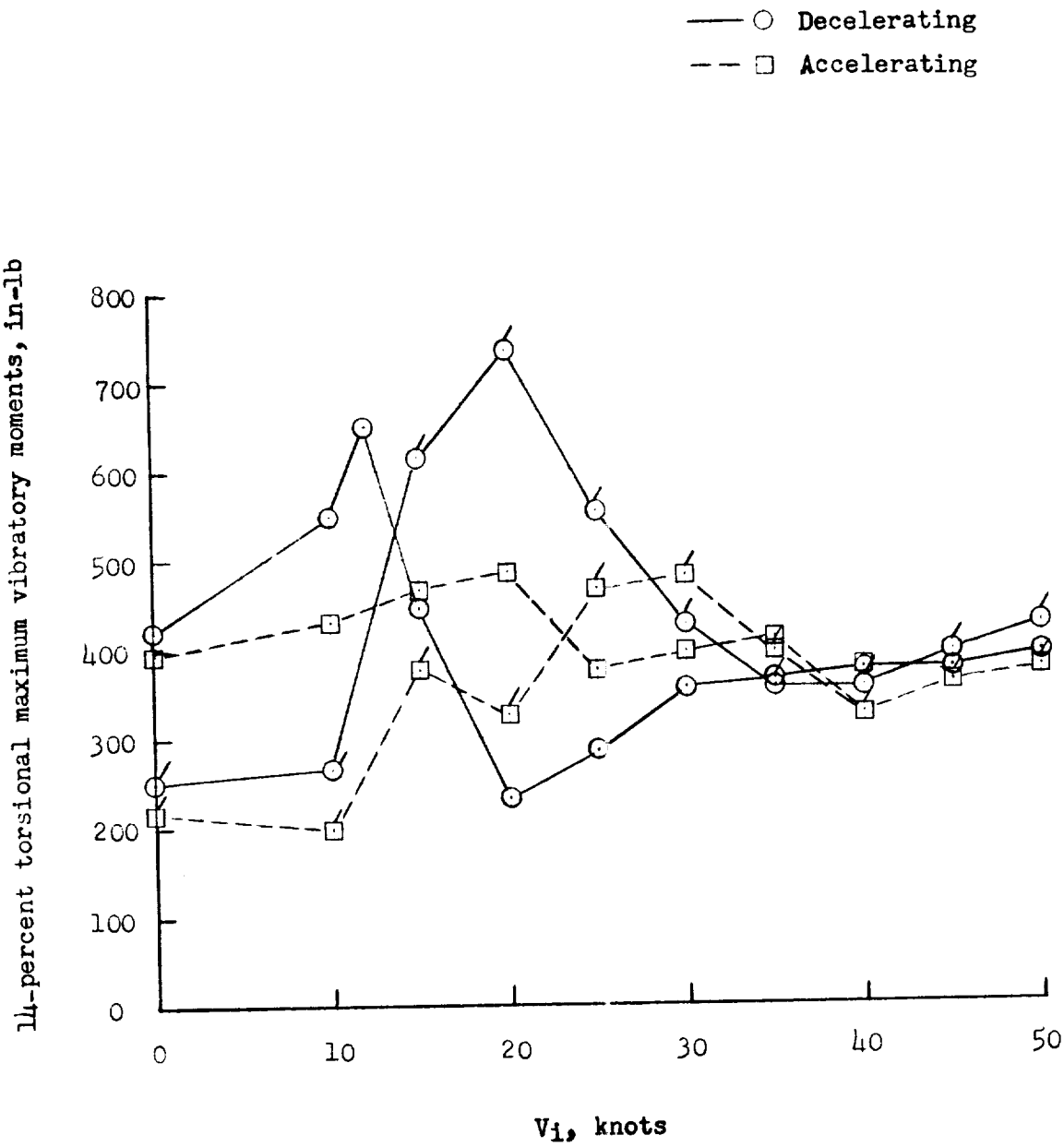

Figure 3.- Concluded.

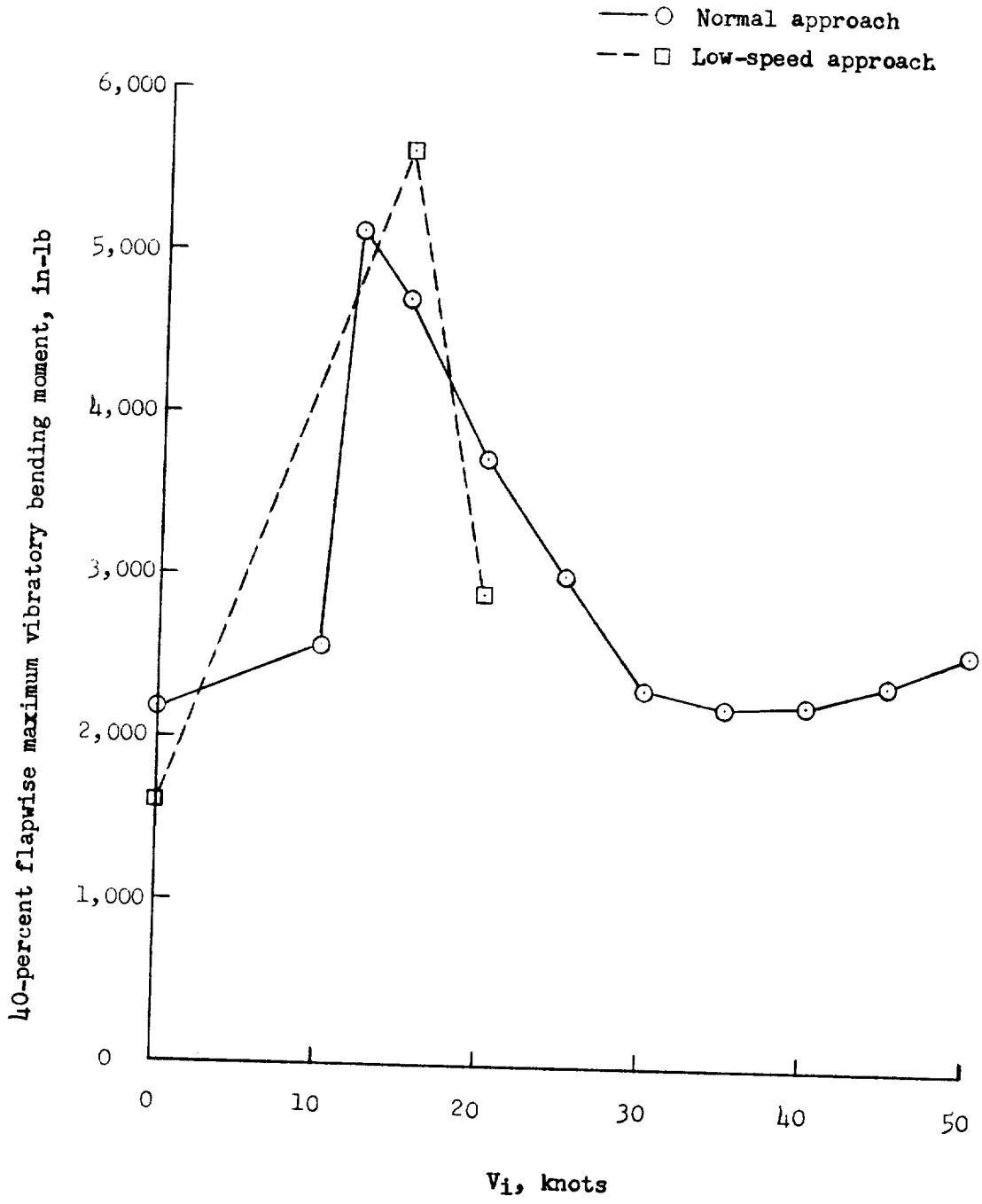

Figure 4.- Effects of landing approaches on the maximum vibratory moments.

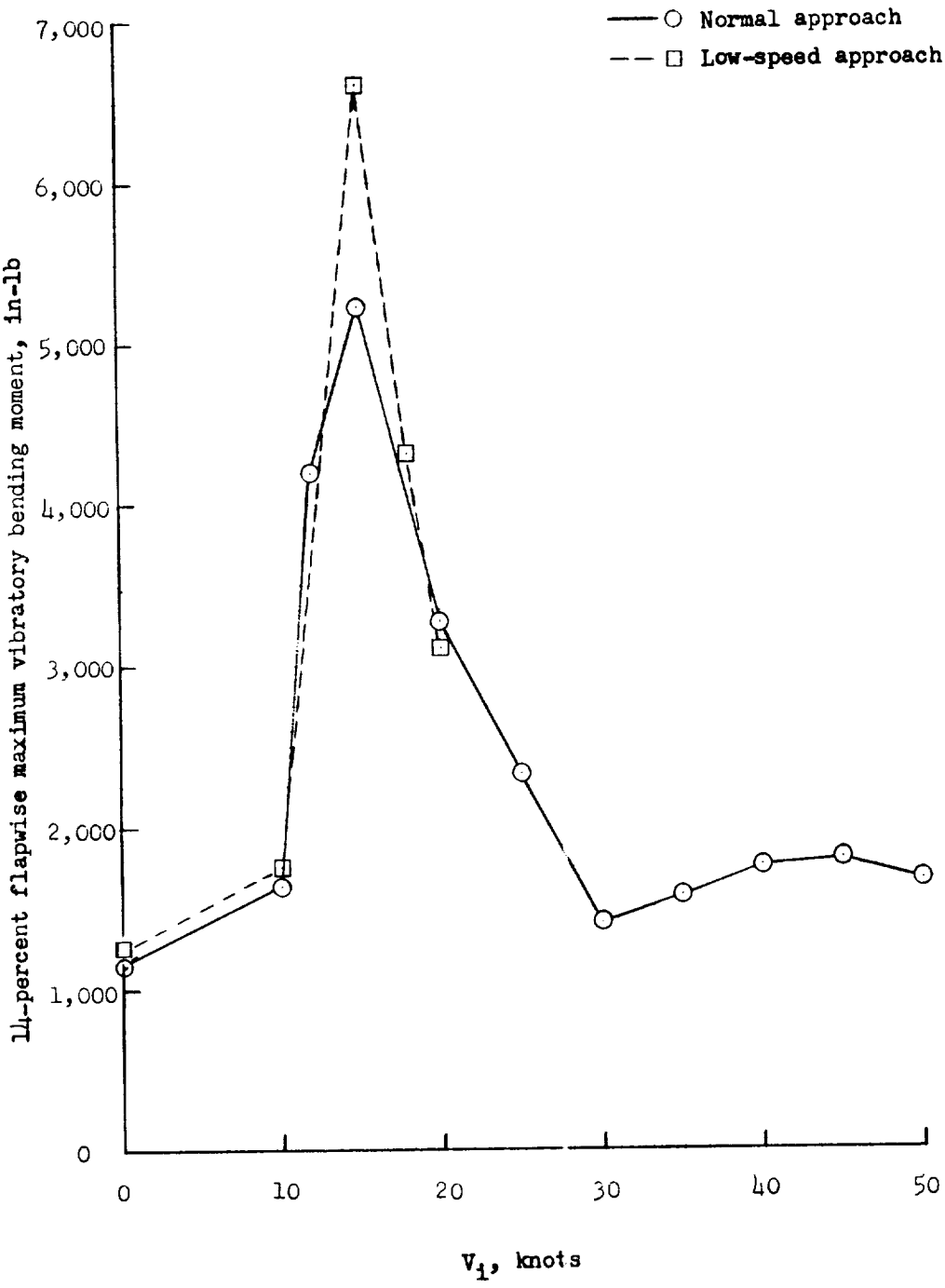

Figure 4.- Continued.

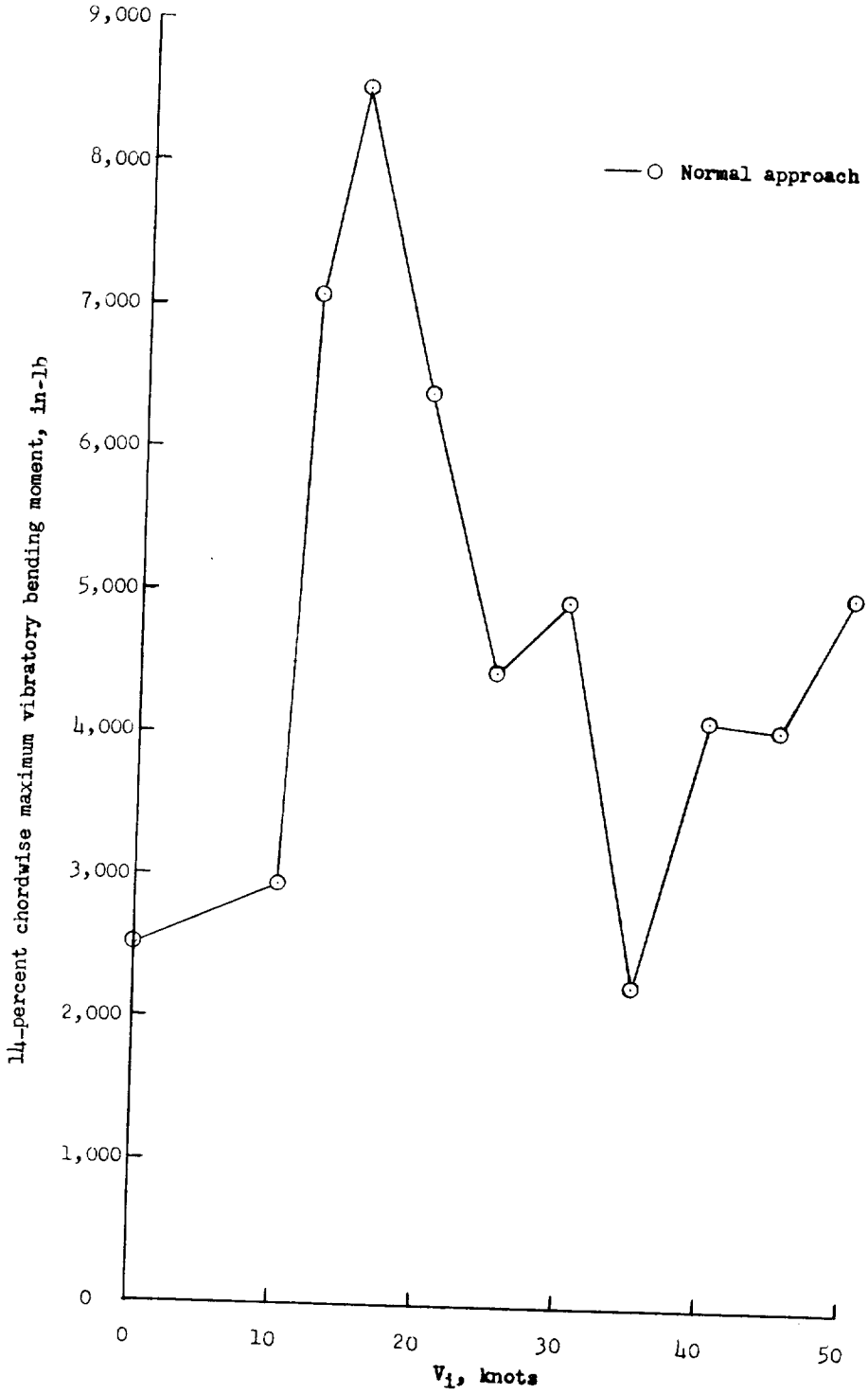

Figure 4.- Continued.

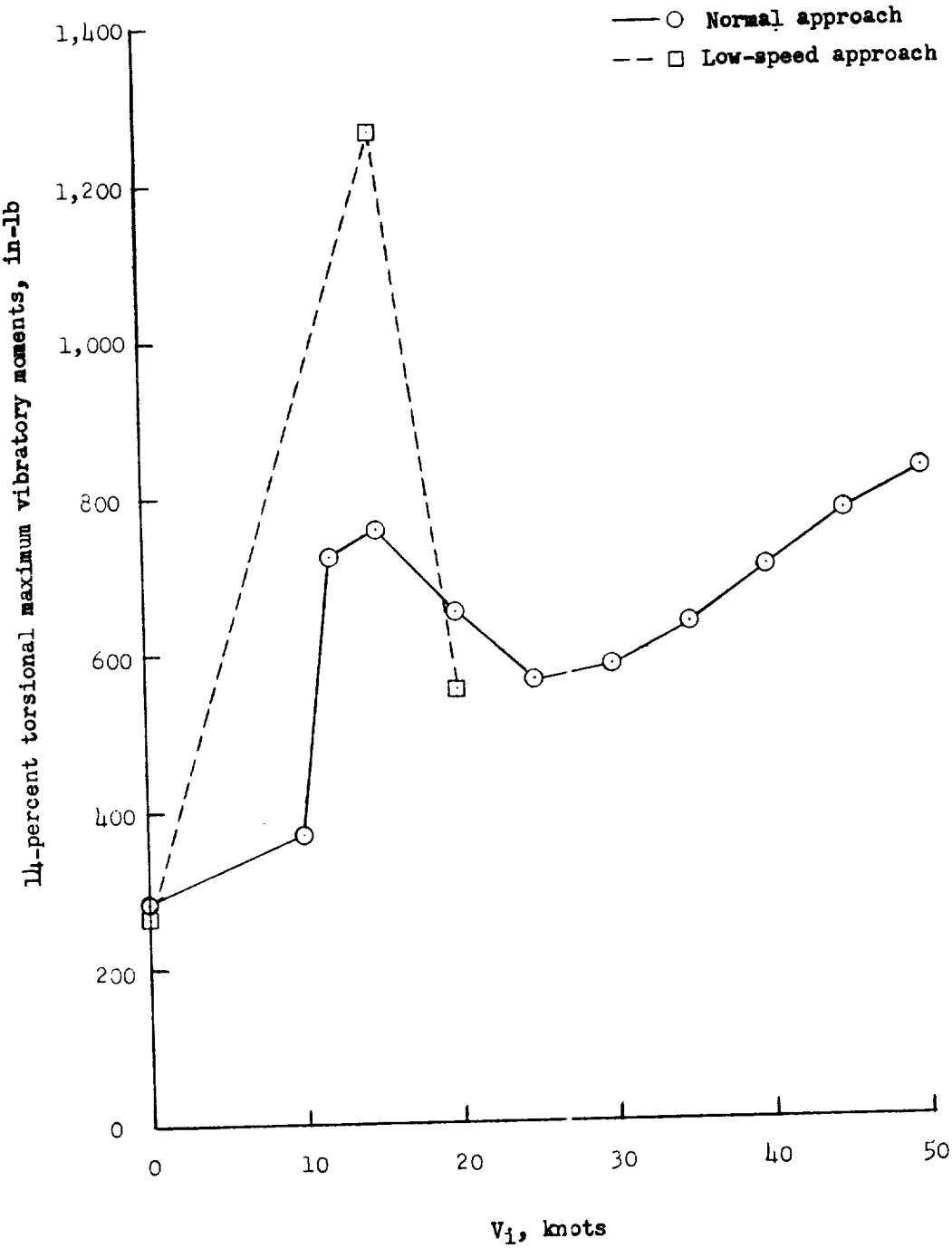

Figure 4.- Concluded.

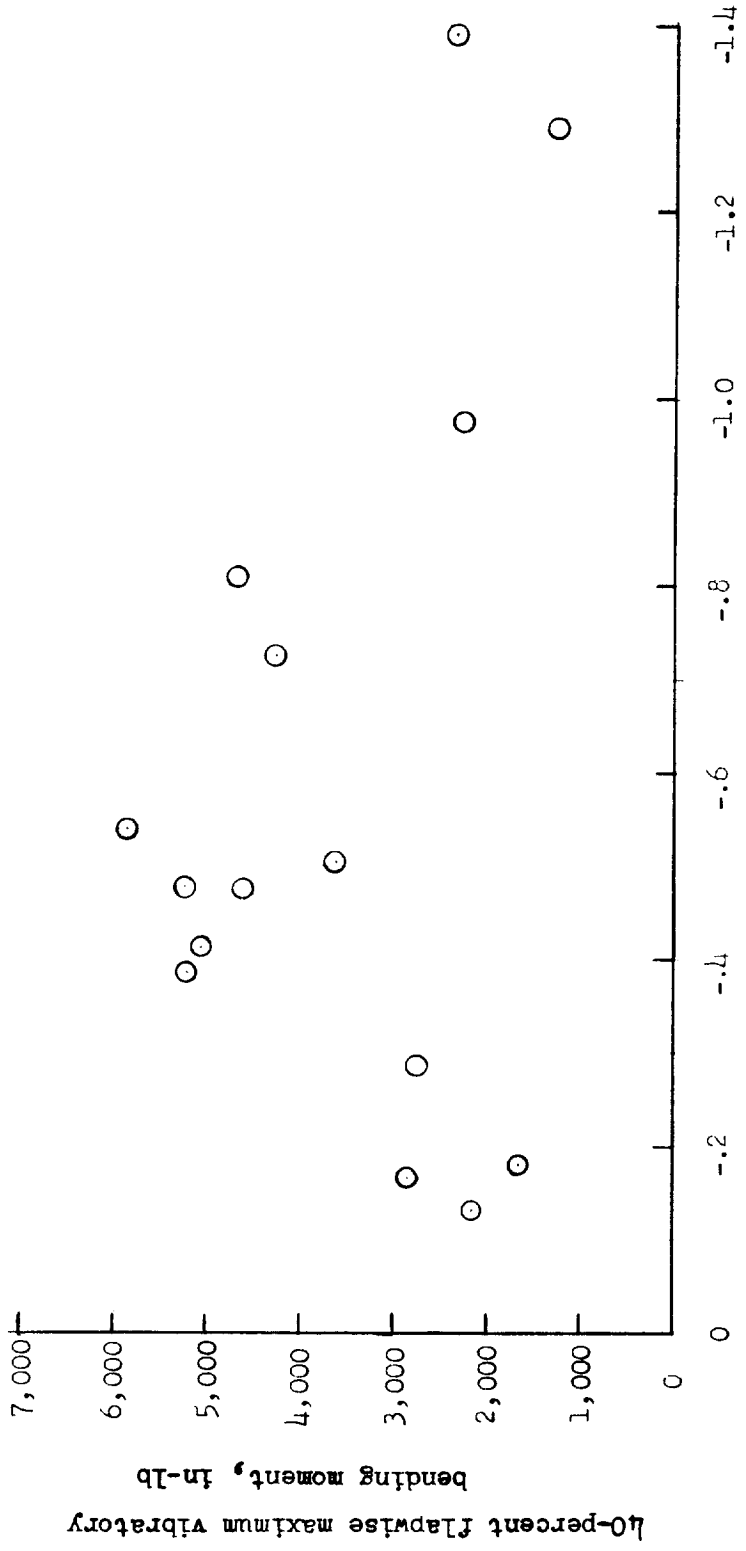

Figure 5.- Effects of partial-power vertical descents on the maximum vibratory moments.

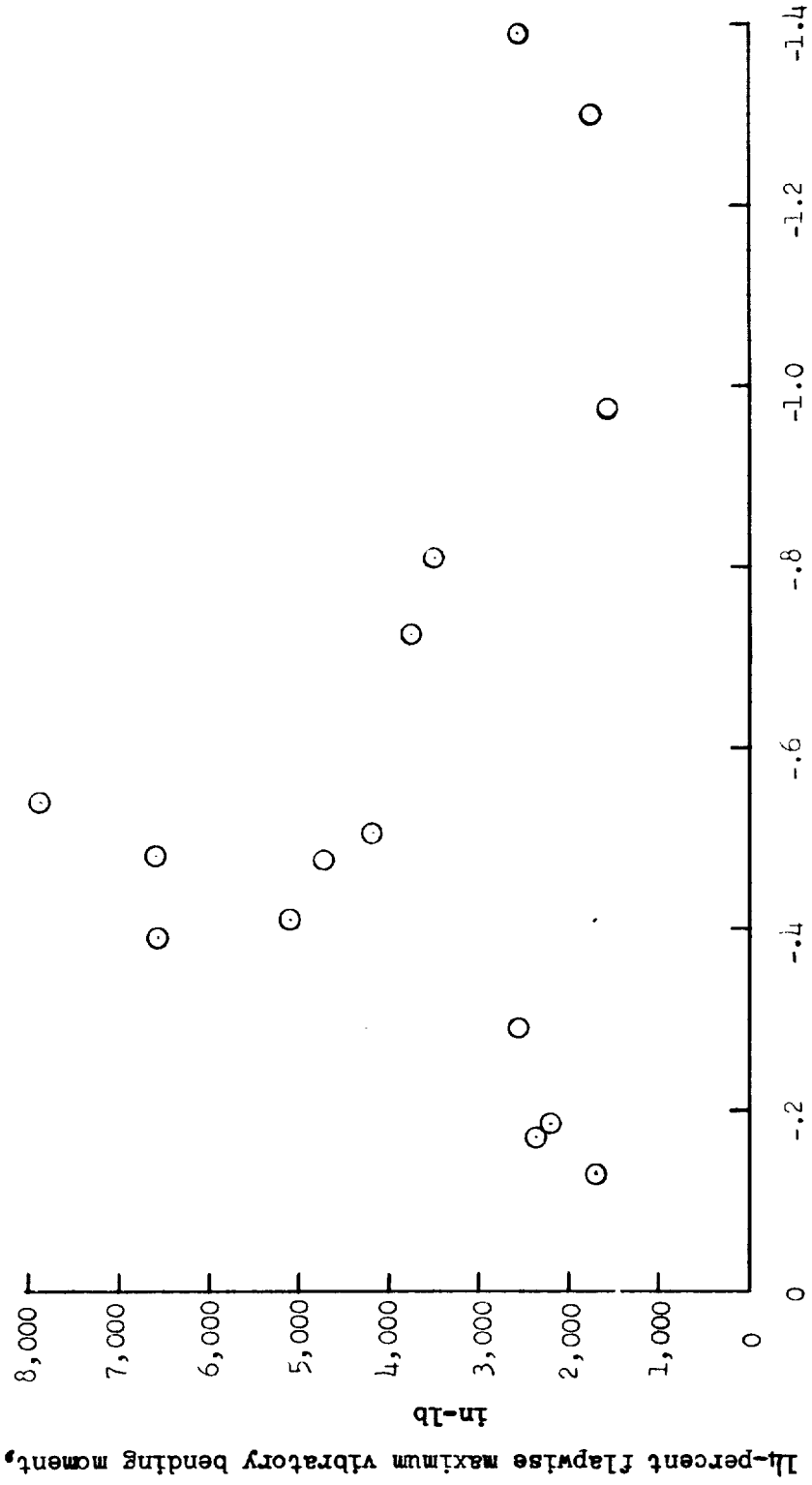

Figure 5.- Continued.

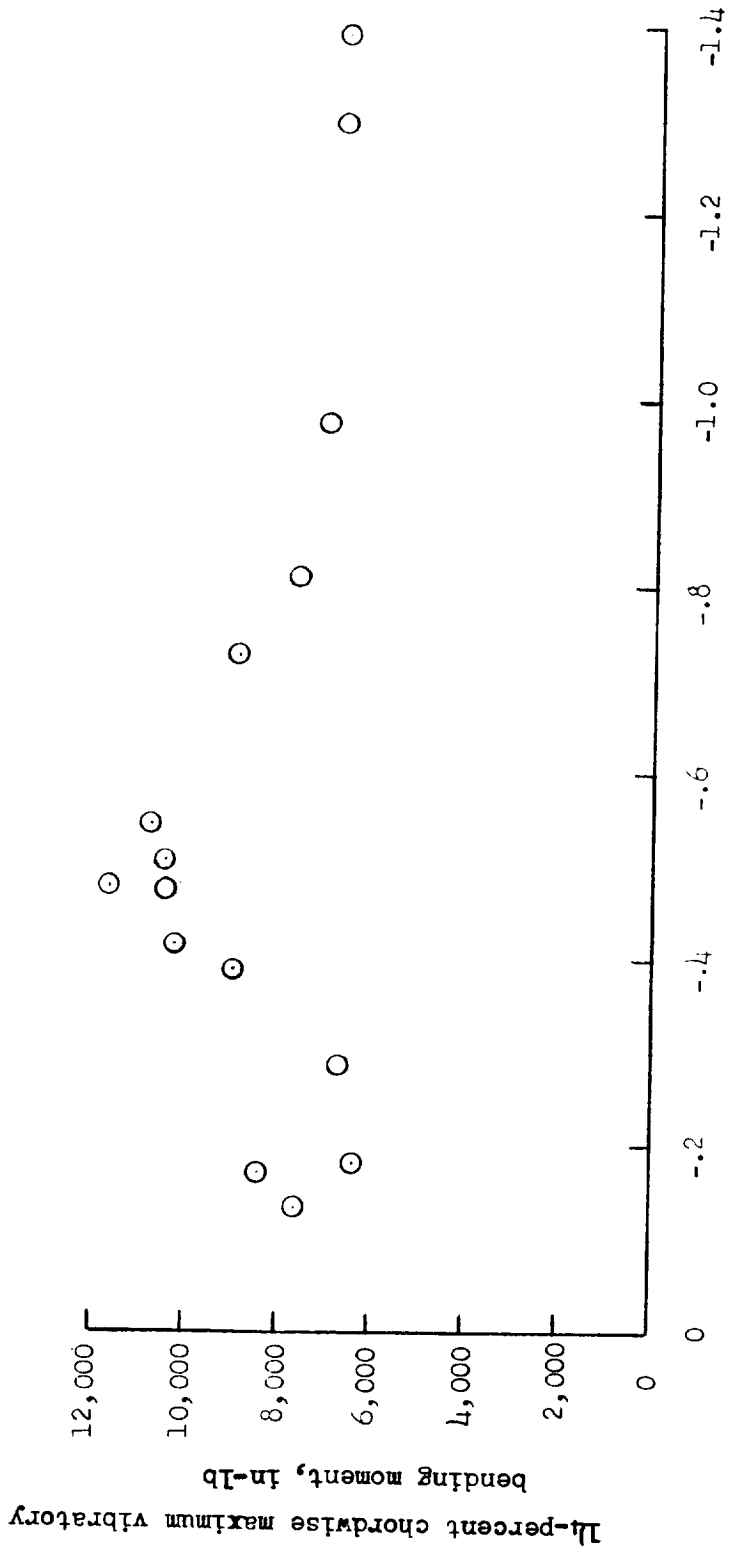

Figure 5.- Continued.

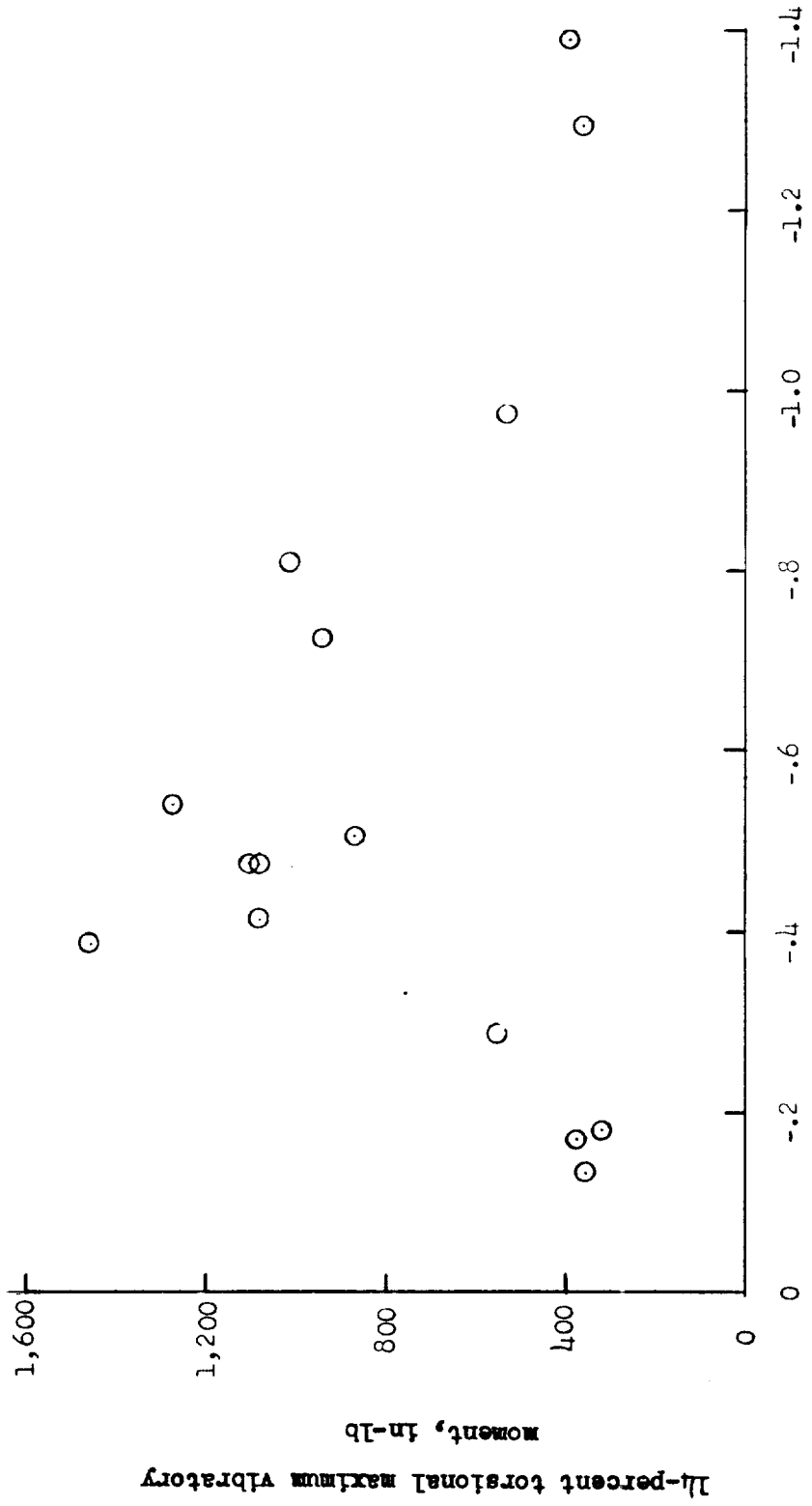

Figure 5.- Concluded.

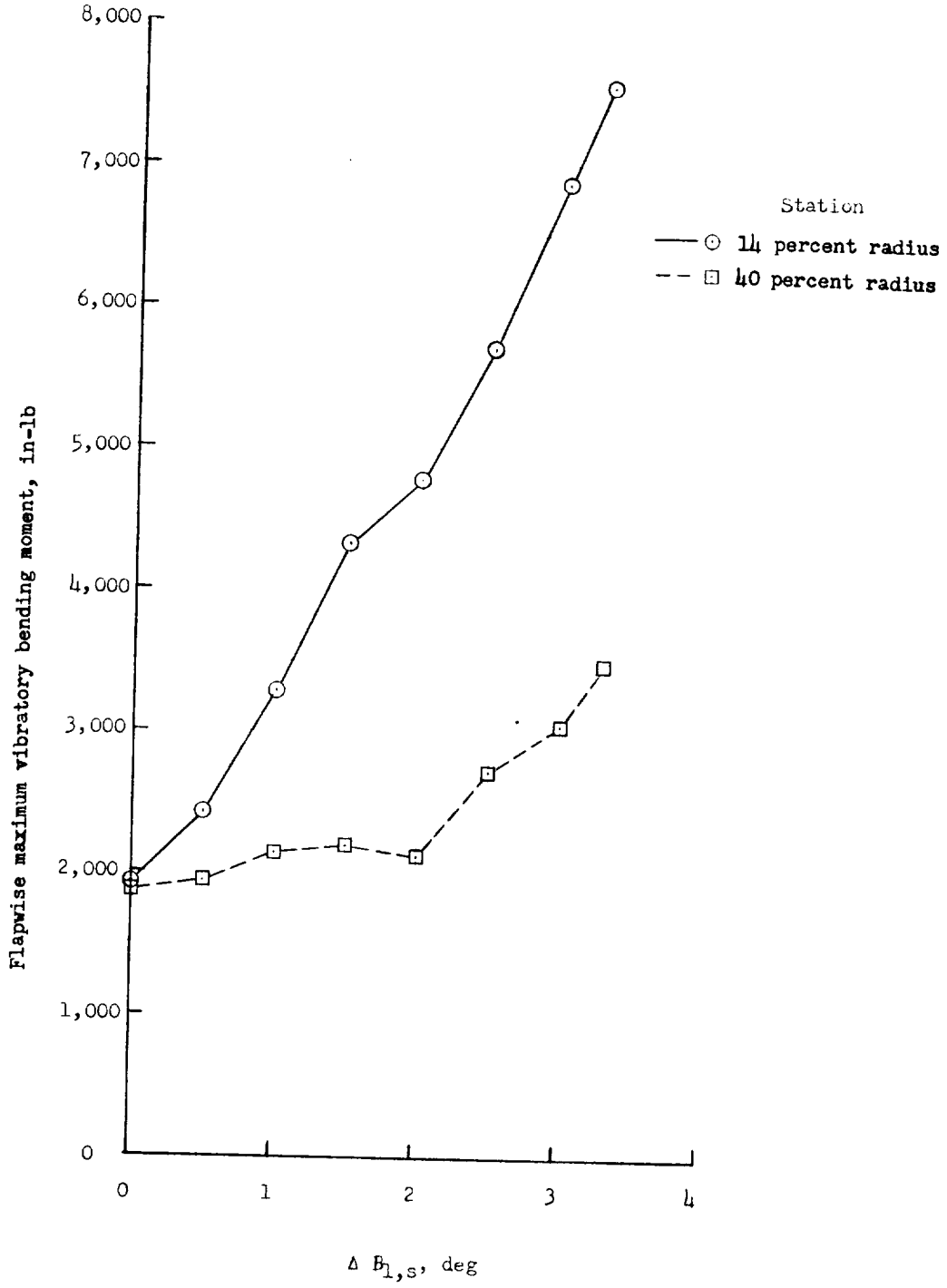

Figure 6.- Effects of static droop-stop pounding on the maximum vibratory moments.

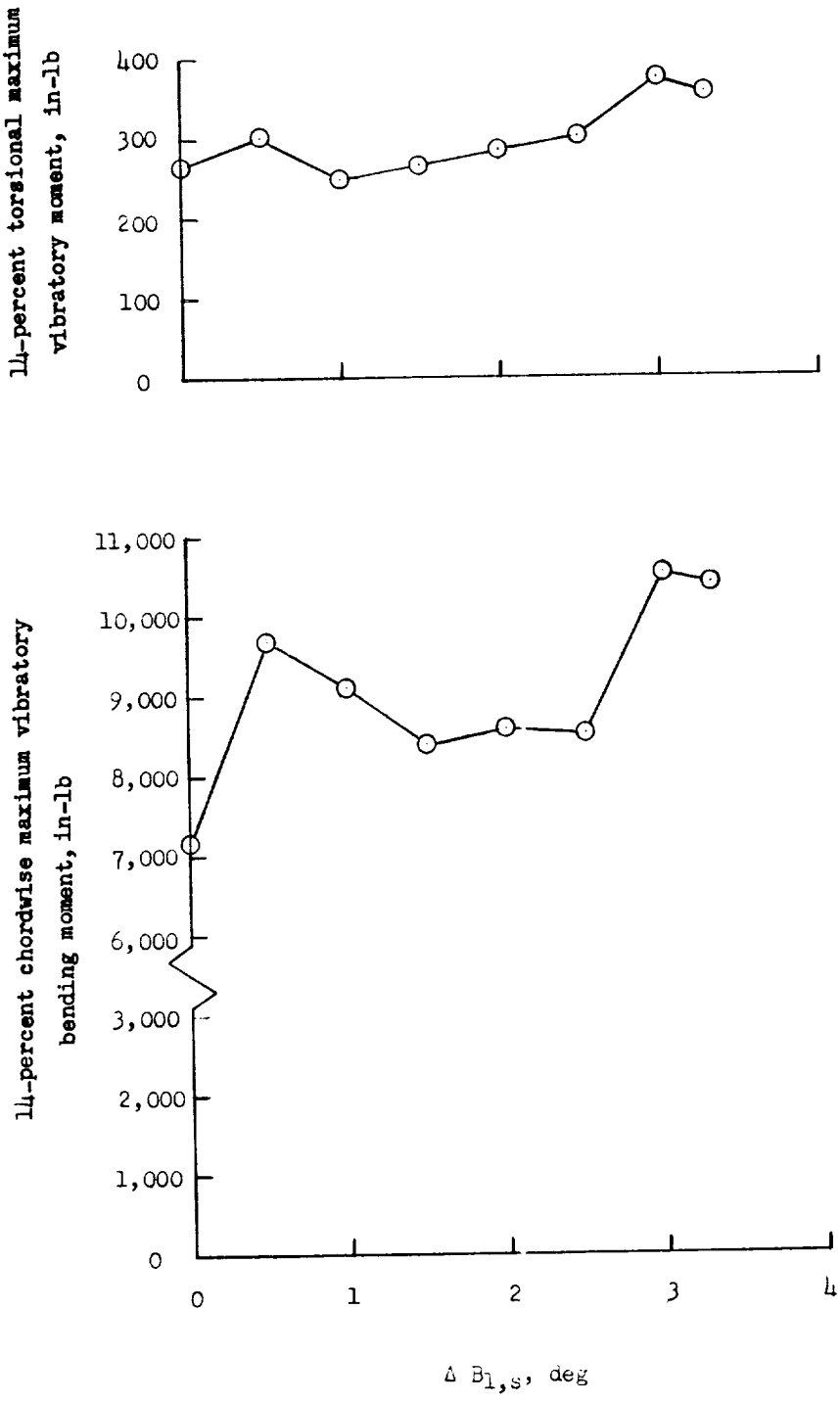

Figure 6.- Concluded.

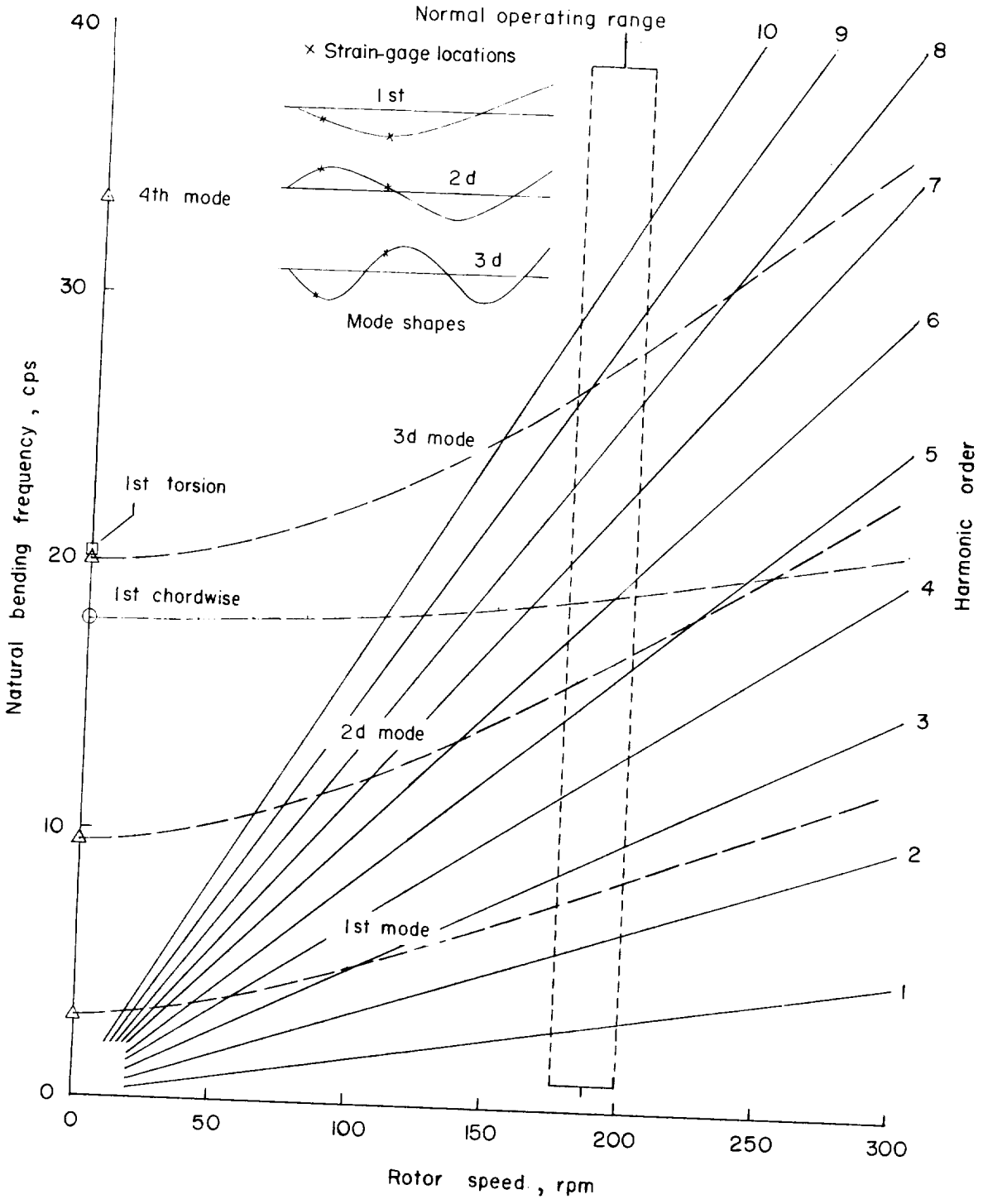

Figure 7.- Rotor-blade-frequency diagram.

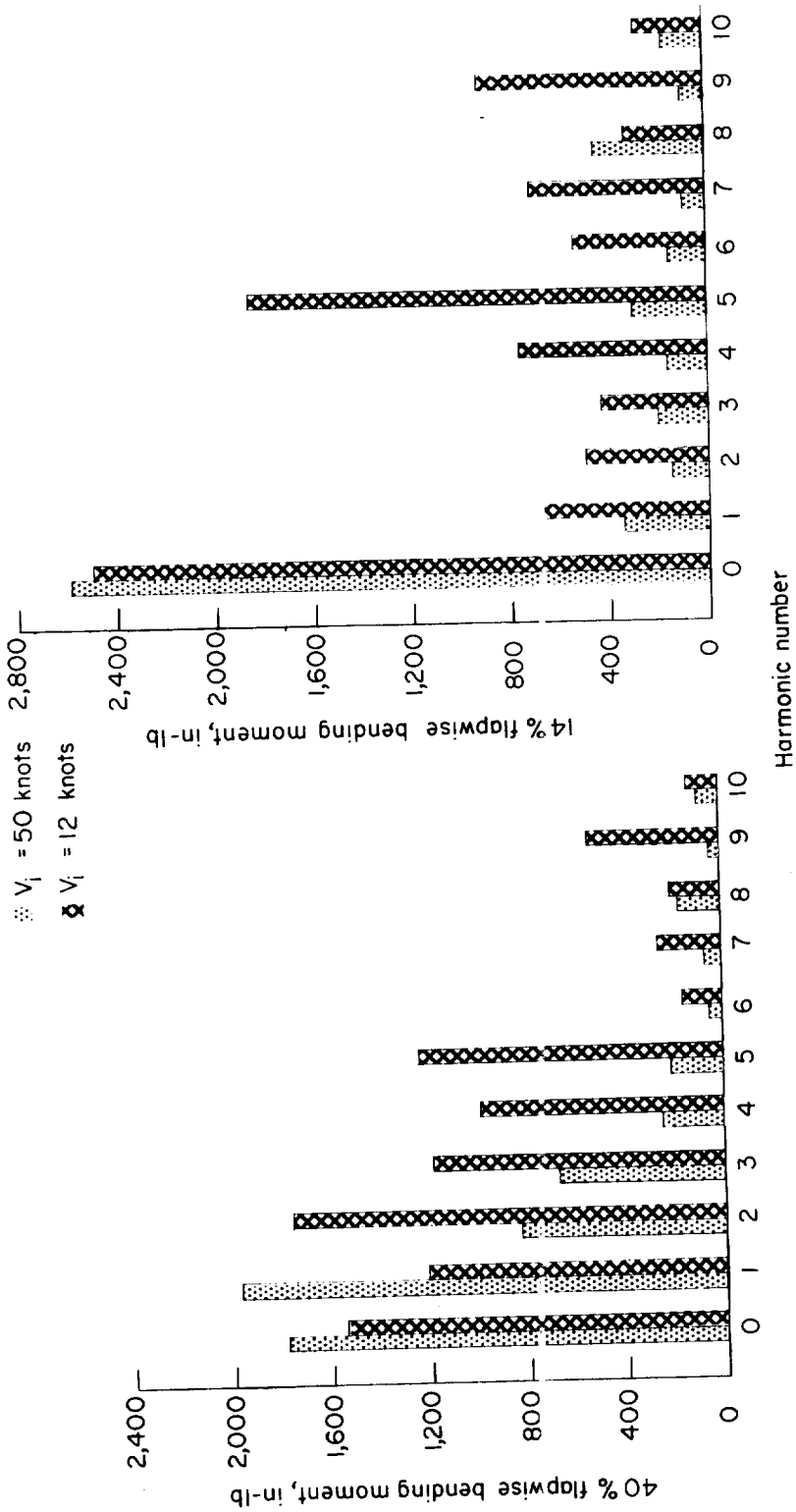

Figure 8.- Effects of decelerating through the transition region (in ground effect) on the rotor-blade moments.

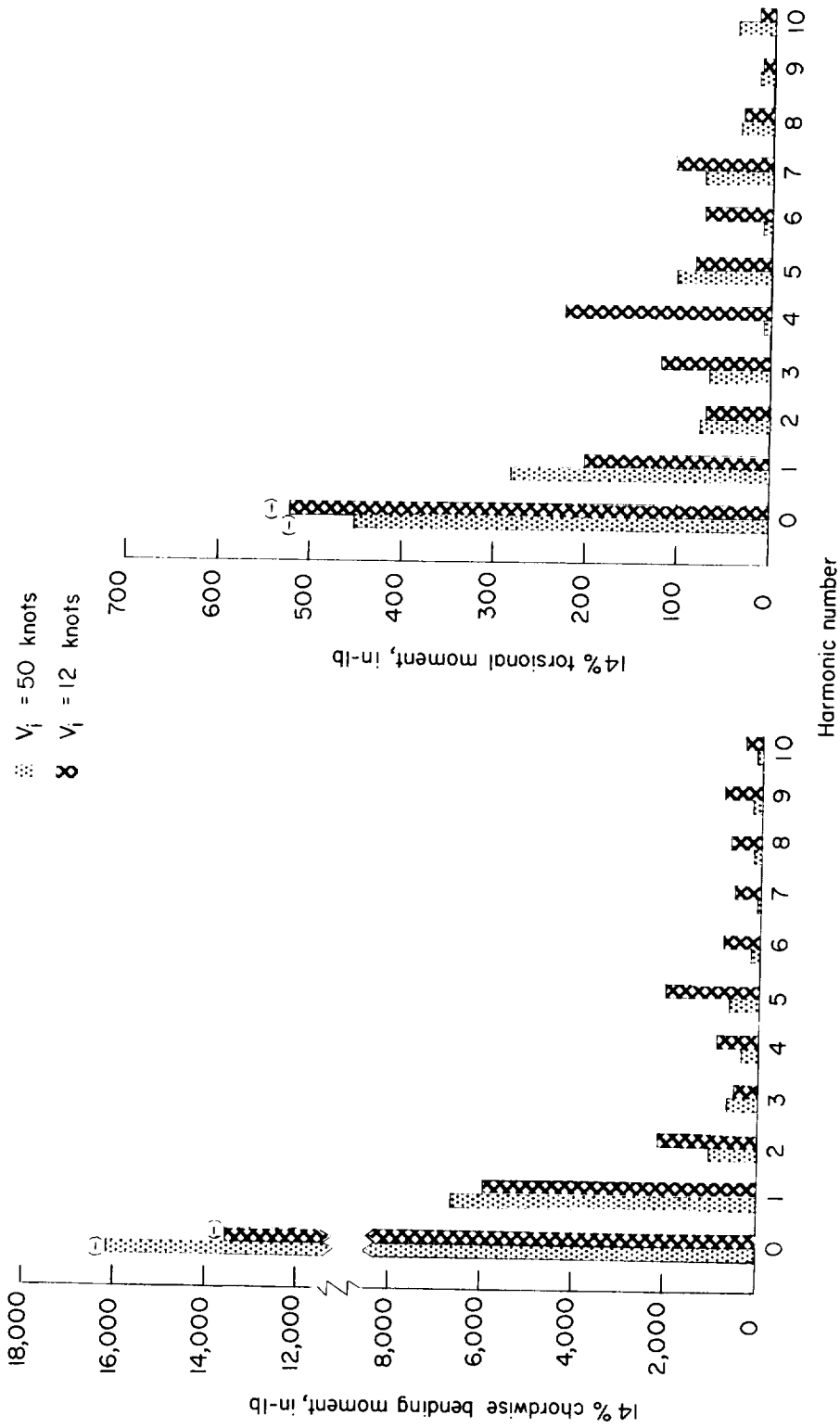

Figure 8.- Concluded.

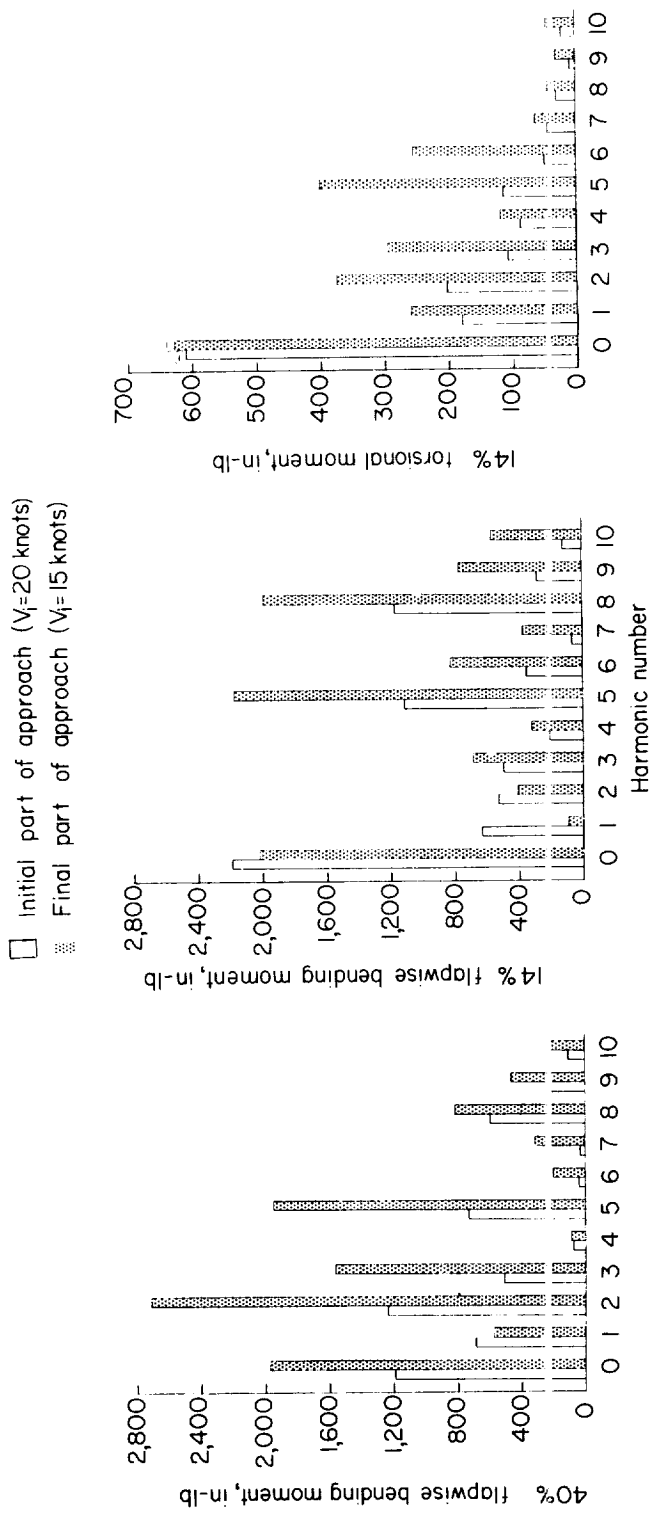

Figure 9.- Effects of low-speed landing approach on the rotor-blade moments.

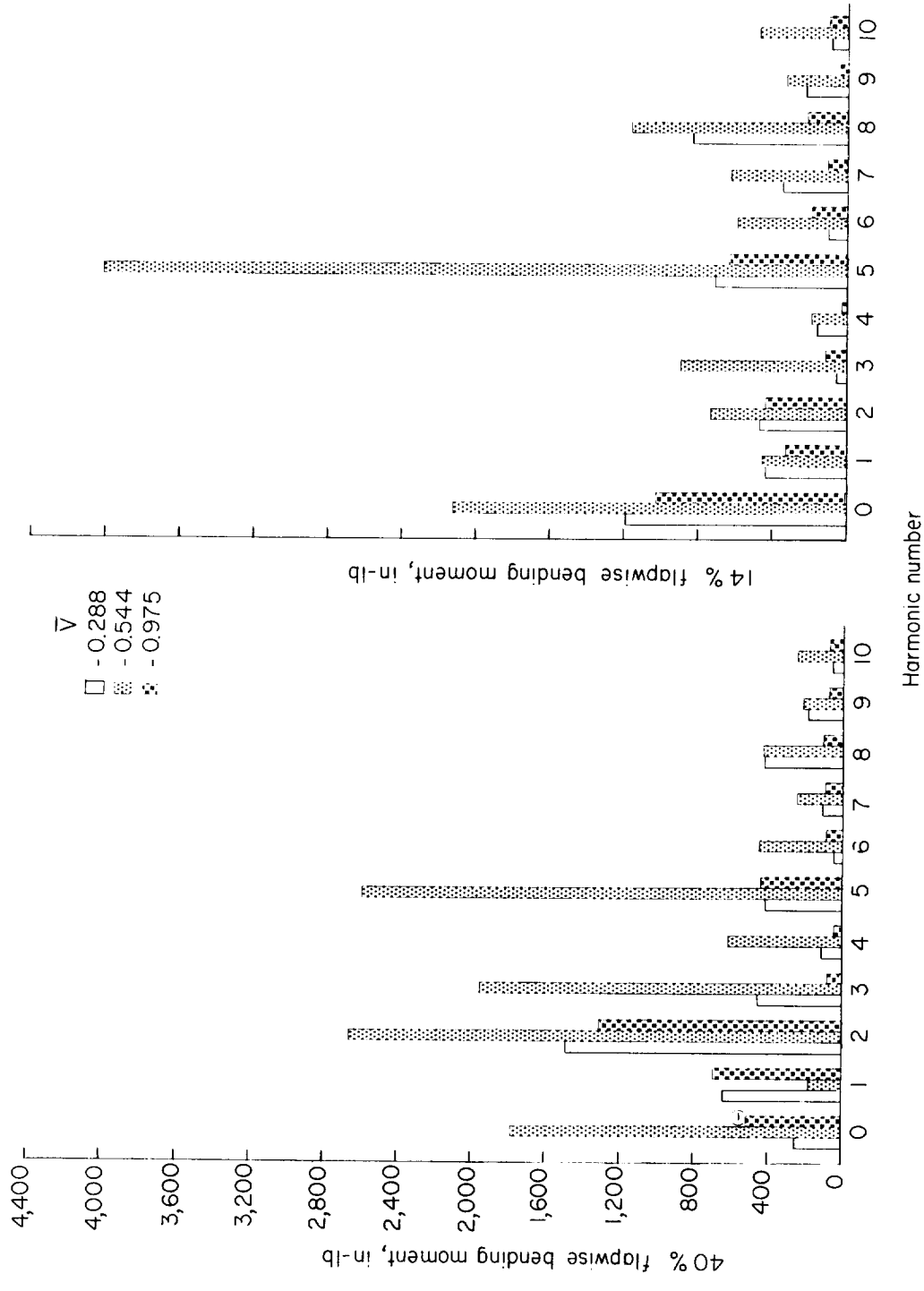

Figure 10.- Effects of partial-power vertical descents on the rotor-blade moments at three different rates of descent.

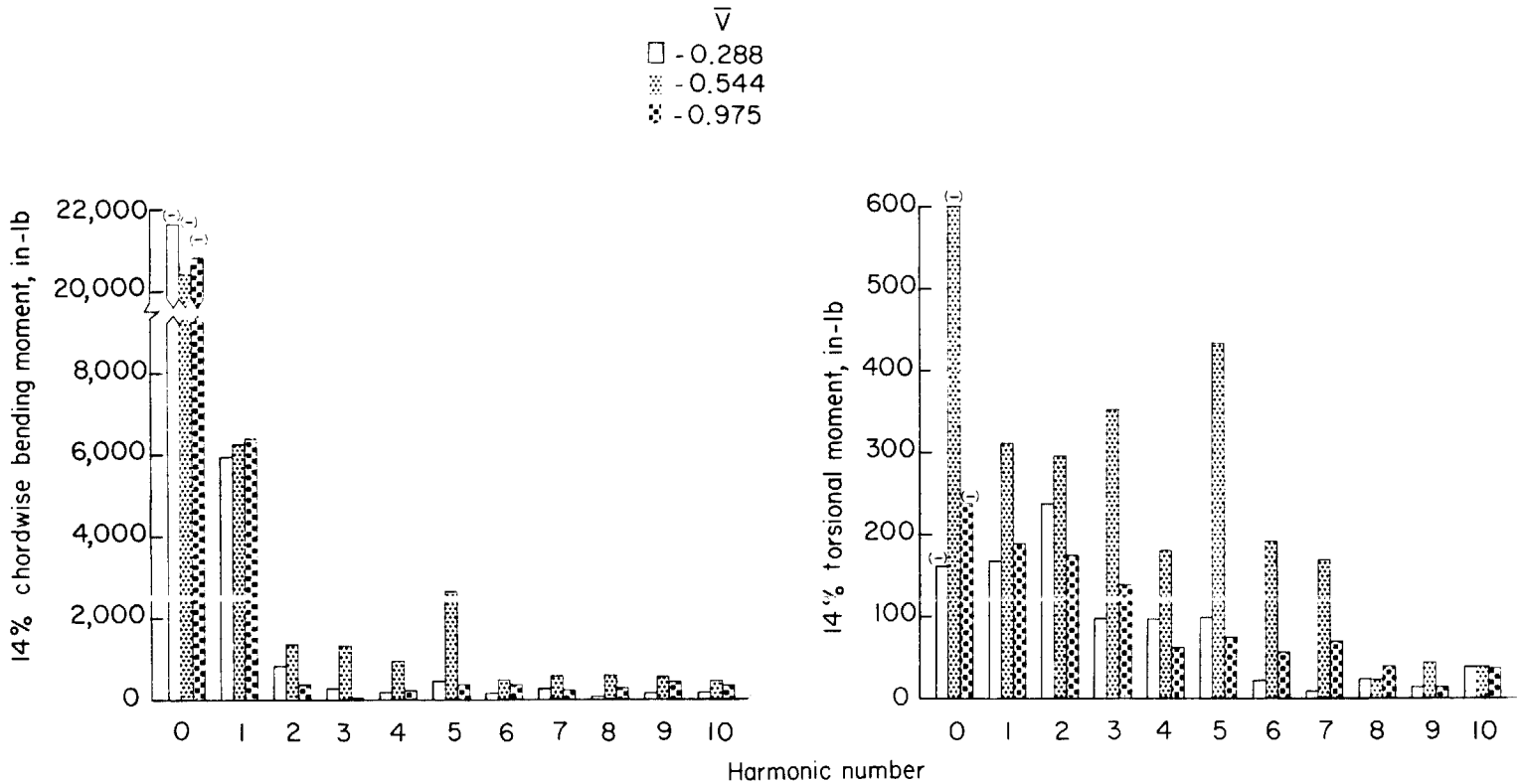

Figure 10.- Concluded.

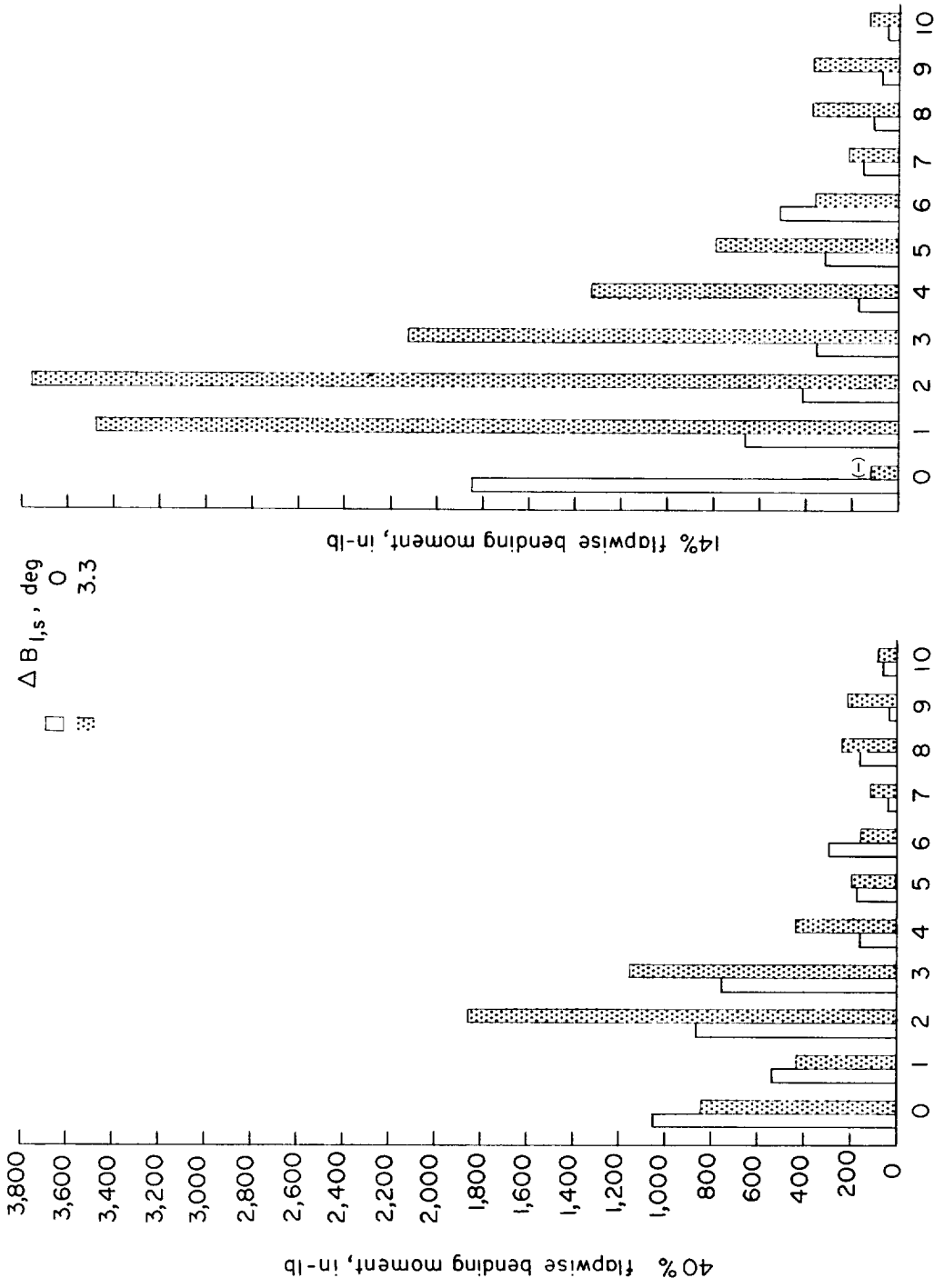

Figure 11.- Effects of static droop-stop pounding on the rotor-blade moments.

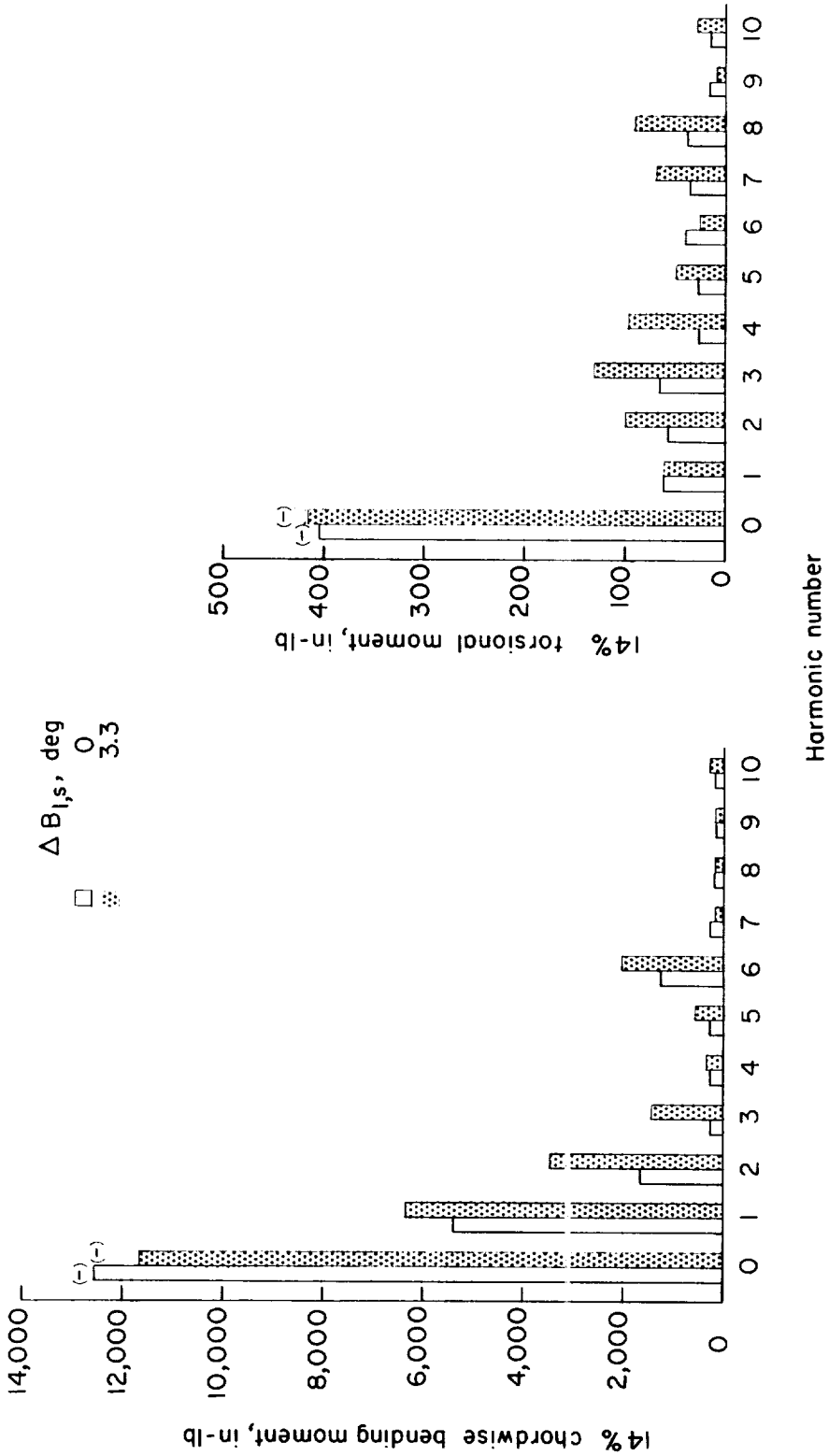

Figure 11.- Concluded.